BLANK PAGES
IN THIS
DOCUMENT
WERE NOT
FILMED

NASA CR-132687

ANALYTICAL EVALUATION OF ILM SENSORS

By Raymond J. Kirk

SEPTEMBER 1975

VOLUME II

APPENDICES

Prepared under Contract No. NAS1-13489 by
HONEYWELL INC.
Systems and Research Center
Minneapolis, Minnesota

for

NATIONAL AERONAUTICS AND SPACE ADMINISTRATION

Analytical Evaluation of ILM Sensors

Volume II

Appendices

Contract No. NAS1-13489

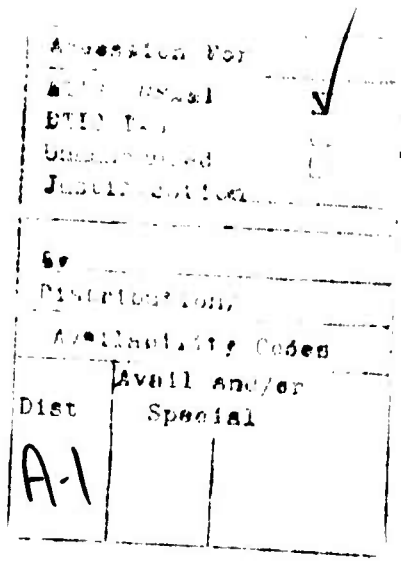

Systems and Research Center
Honeywell Inc.

SECTION IX

APPENDICES

APPENDIX A. TENTATIVE MLS ACCURACY REQUIREMENTS

GENERAL

Safe flights and landings generally require the following aircraft performance:

- o The aircraft path deviations should be within safe limits.
- o The aircraft path rates (such as sink rate) should be within safe limits.
- o The aircraft attitude changes should be comfortable to pilot and passengers.
- o The aircraft control surface movements should be within reasonable mechanical limits and should allow adequate margins for response to air turbulence and other factors.
- o The aircraft control column activity should be comfortable to the pilot.
- o For manual flight the display activity should be acceptable to the pilot.

The MLS shall not compromise the ability of the aircraft to maintain these criteria.

The factors of error magnitude, duration, spectral content and zone of occurrence are important as well as the factors of aircraft type, AFCS configuration, gain, and transient response.

Angle Noise (Includes Receiver Noise) -- Angle noise is defined as spatial and temporal perturbations in the guidance signal. It originates from both ground and airborne equipment and the environment.

Path Following Noise -- Path following noise is defined as that portion of angle noise which can cause aircraft motion; it exhibits relatively slow variations.

Control Motion Noise -- Control motion noise is that portion of angle noise which affects control surface, wheel, column motion, and aircraft attitude; it exhibits moderately fast variations.

Extraneous Noise -- Extraneous noise is that angle noise which exhibits variations too rapid to affect aircraft control and guidance.

Path Following Error -- Path following error is defined as the angular deviation from a predetermined course of an aircraft perfectly following MLS guidance commands. The error is thus due to angle bias and path following noise in the guidance signal.

Range Error -- The range error is the difference between the suitably processed DME range and the true distance at any given point in time. DME bias and noise errors have the same general definition as for angle guidance.

Course Linearity Error -- Course linearity error is the deviation of the angle coding scale factor from the nominal, about a selected course. Linearity errors affect effective AFCS gain and display sensitivity, and con-

o High - Does not affect aircraft control and guidance.

In terms of spectral density, the bias would be lower frequency limit of noise (approximately 0 to .05 radians/second for a 60-second record).

While the term "path following error" suggests the difference between a desired flight path and the actual flight path taken by an aircraft following the guidance, in practice this error is estimated by instructing the test pilot to fly a desired course, and measuring the difference between the filtered guidance indication and the corresponding position measurement determined by a high-accuracy instrument such as a theodolite. The errors and spectral distribution thus obtained give an accurate estimate of the path following parameters. A similar technique is used to determine the control motion noise.

Treatment of Sudden, Large Errors

Interference or multipath can occasionally cause large, sudden changes in angular indication. Provision shall be made to handle such transients while maintaining validation and coast requirements. Capability of "coasting" through periods of transients shall be provided, which rejects loss of data for a period of time up to 2 seconds, except that those functions, actively in use to determine flare altitude, shall be limited to 0.5 seconds coasting time.

Bias

The angular bias is determined by averaging the time error record of a test flight (the difference between the MLS-derived angle and the tracker-derived angle) over a period of 60 seconds.

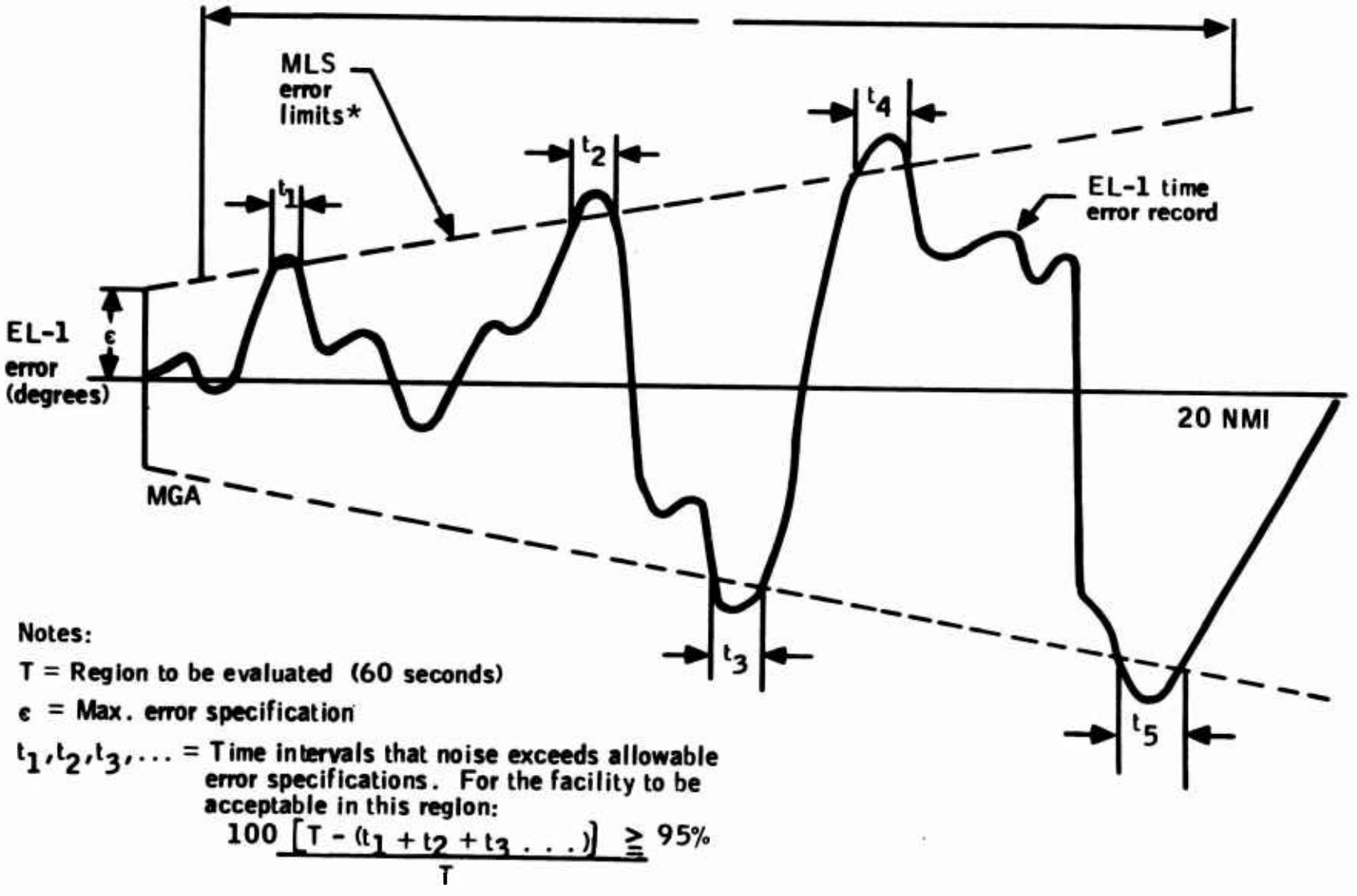

Notes:

T = Region to be evaluated (60 seconds)

ϵ = Max. error specification

$t_1, t_2, t_3, \ldots$ = Time intervals that noise exceeds allowable error specifications. For the facility to be acceptable in this region:

$$100\,\frac{\left[T - (t_1 + t_2 + t_3 \ldots)\right]}{T} \geq 95\%$$

Figure A-1 -- Time Error Record Analysis of Path Following Filter Output and Control Motion Filter Output

Table A-2 -- Control Noise Specification

Antenna signal	Noise (2σ)	Allowable degradation		
		With distance	With azimuth angle	With elevation angle
Azimuth	0.04°	1.4:1 at 20 nmi	None	None
Elevation	0.05°	1.4:1 at 20 nmi	None	None
DME	40 feet	10:1 at 20 nmi	None	None
Flare	.02	1.5:1 at 5 nmi	None	None

ERROR INTERPRETATION

Procedures are outlined below which relate the measured parameters to the specification for accuracy. Refer to Figure A-3 for definition of points outlined below and to Table A-4 for the filter configurations.

Point A: MLS Raw Error Data.

Point B: Time Average over any 60-second Portion of Flight Course. Course Bias - See Table A-1 for limits.

Point C: Path Following Error; see Table A-1 for limits; use technique described in Figure A-1 for calculation.

Point D: Use Table A-2 for limits.

Data Rate: The MLS signal format shall accommodate different data rates in different configurations. The format shall be capable of providing the minimum information update rates for the functions in each configuration as shown in Table A-3.

TABLE A-3. MLS MINIMUM INFORMATION UPDATE RATES

FUNCTION	UPDATES PER SECOND
All angle functions except Flare	5
Flare	10
Aircraft Carrier Landing -	
Azimuth	10
Elevation	10
DME Interrogation Rate -	
Normal	40
On-Ground	5
NOTE: All numbers update per second	

Table A-4 -- Filter Configurations and Corner Frequencies

Guidance function	Corner frequencies (radians/sec)					
	ω_0	ω_1	ω_2	ω_3	ω_4	ω_5
AZ	.05	0.3	10	2	4	.05
El	1.5	0.5	10	2	4	.05
Flare	2.0	0.5	10	2	4	.05
DME	10	0.5	10	TBD	TBD	.05

Filter configurations

Smoothing filter $\dfrac{\omega_2}{S+\omega_2}$

Path following filter $\dfrac{\omega_n^2}{S^2+2\xi\omega_n S+\omega_n^2}$; $\xi = 1$; $\omega_0 = .64\omega_n$

$$\omega_0=\omega_n \sqrt{1 - 2\xi^2 + (4\xi^4 - 4\xi^2 + 2)}^{1/2}$$

Control Motion filter: $\dfrac{S}{S+\omega_1}$

Rate filter: $\left(\dfrac{S}{S+\omega_3}\right)\left(\dfrac{\omega_4}{S+\omega_4}\right)$

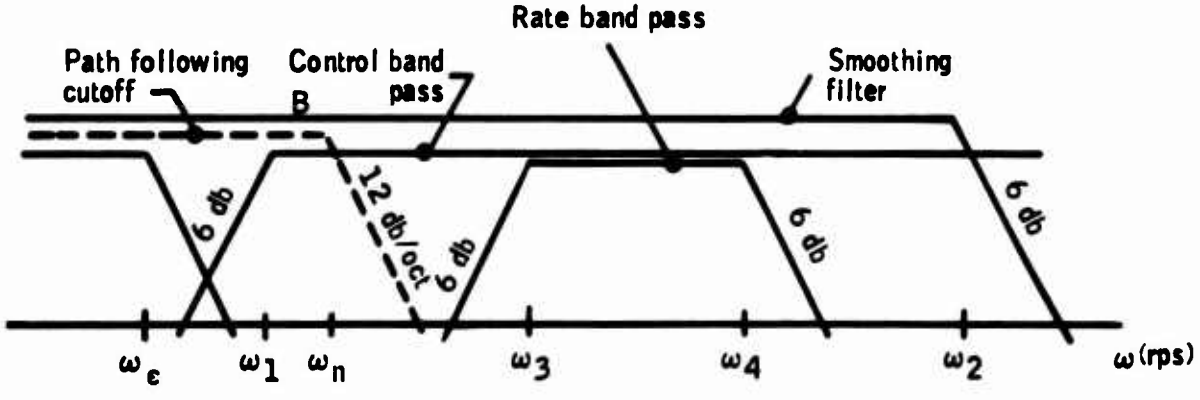

APPENDIX B. MARSAM II COMPUTER PROGRAM SUMMARY

INTRODUCTION

The overall purpose of the MARSAM II program was to develop and implement a mathematical computer model for use in the performance assessment of reconnaissance sensor systems of varied types operating on prescribed aerial flight profiles against ground targets in specified background and weather environments. MARSAM II (the mathematical model acronym) addresses those aspects of sensor performance as are related to the capability of such systems to provide target identification detail. Specifically, the types of aerial sensor systems considered in the MARSAM II model are: frame and panoramic cameras, television, the visual observer, vertical and forward-looking infrared, side-looking and forward-looking radar, and ELINT. As applicable to the different sensor types, film record and/or display modes of operation are considered. In addition, there is provided as an integral part of the MARSAM II computer model a stored library of characteristic data for numerous target-elements, backgrounds, and weather conditions (such data is readily expanded or modified by the user analyst). Where the provided library data base is considered applicable to a given problem, the task of preparing model inputs is significantly eased for the user. Available outputs from MARSAM II range from detailed sensor system performance parameters and associated probability measures of detection, recognition and identification to mission success measures. The MARSAM II computer model was developed as a tool for use by sensor systems design analysts in their

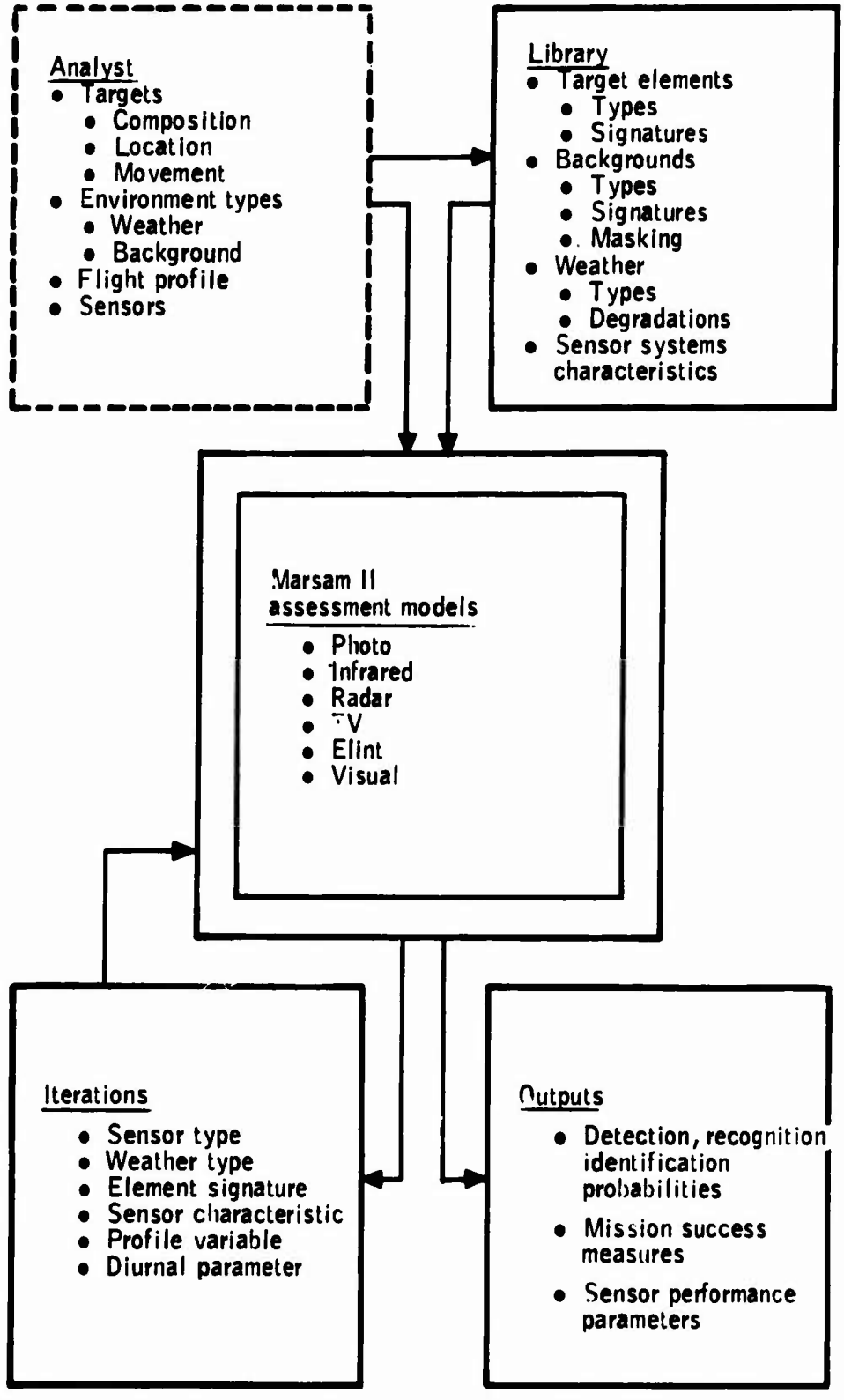

Figure B-1 -- MARSAM II Capabilities Summary

Simplification of model use results from availability of a library of target-element*/environment/sensor-system characteristic data, such library data base being an integral part of MARSAM. To input a problem to the model, the analyst describes target composition by a code number for each of the target elements within the target. Similarly, atmospheric and background environment characteristics may be input, in the main, by specification of code numbers. Thus, such code number inputs are used as the means to obtain from the library and input to the model a majority of the required target-element, enviroment, and sensor-system characteristic data (library data is readily expanded or modified as desired by the analyst).

Further simplification and efficiency of model use results from the automatic manner of sensor-to-target offset consideration. That is, for a specified sensor and specified flight speed and altitude, the model automatically determines and assesses sensor performance at only those aircraft-to-target offset distances for which at least one target element falls within the sensor field of view.

* In the vernacular of MARSAM, a target is defined as a group of one or more target elements where, for example, a target element may be a man, a truck, a boat, a hangar, a surface opening, etc.

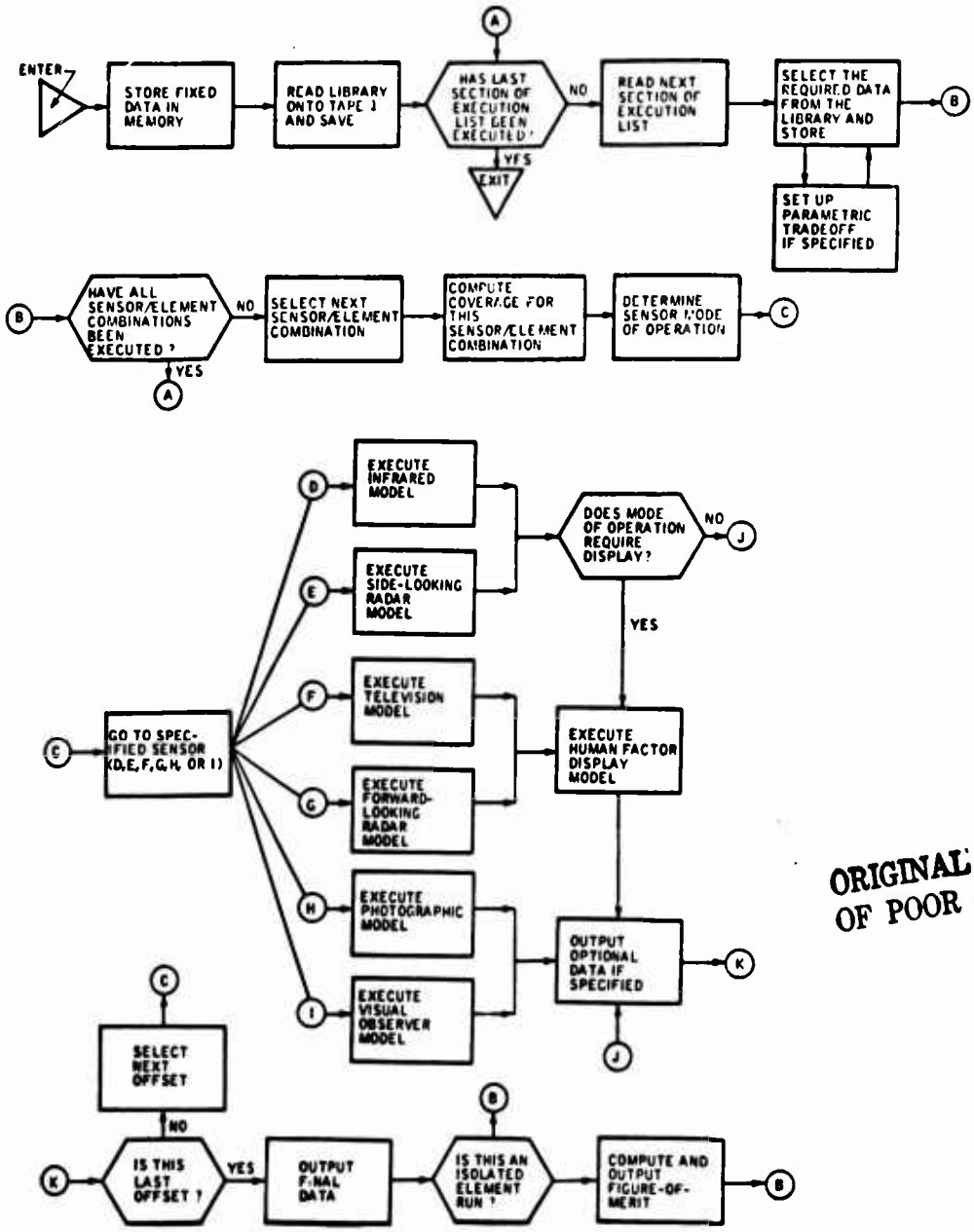

Figure B-2 --MARSAM Program Information Flow

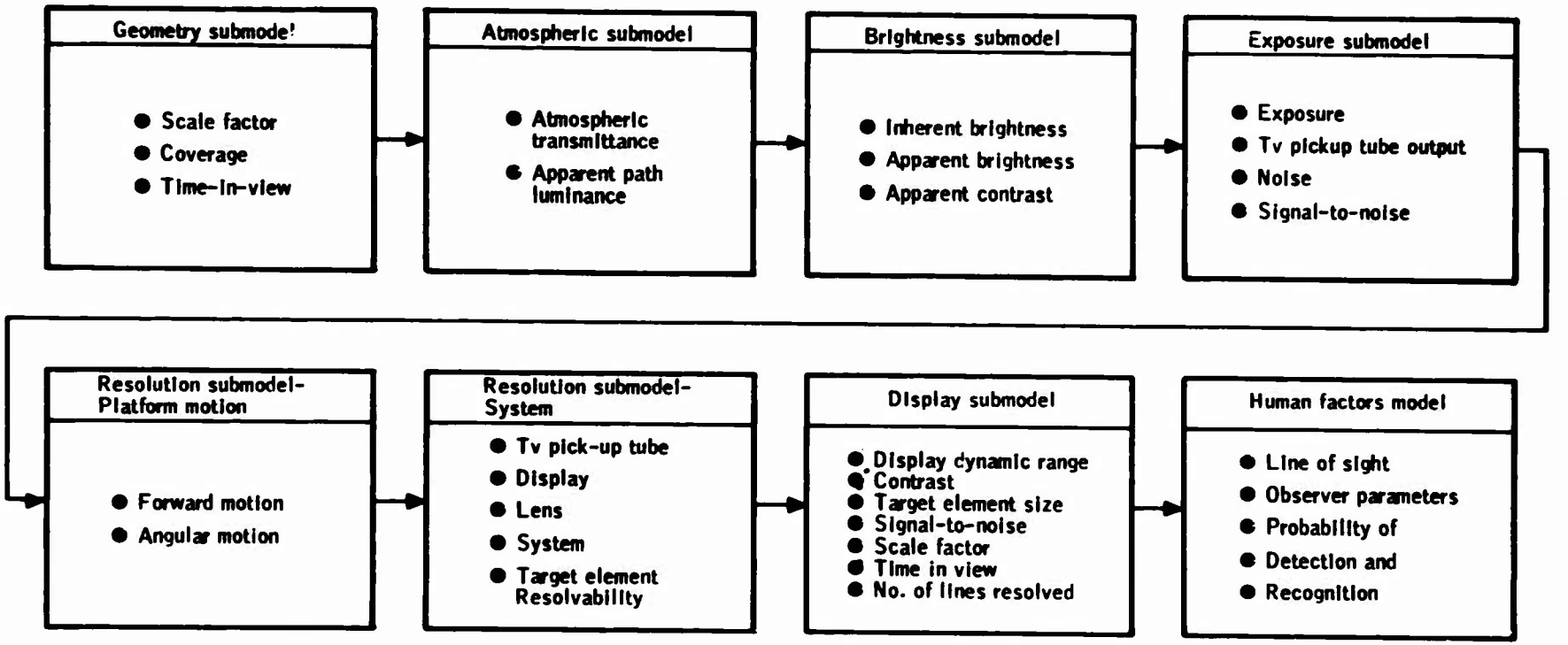

Figure B-3 -- Television Sensor Model Data Flow

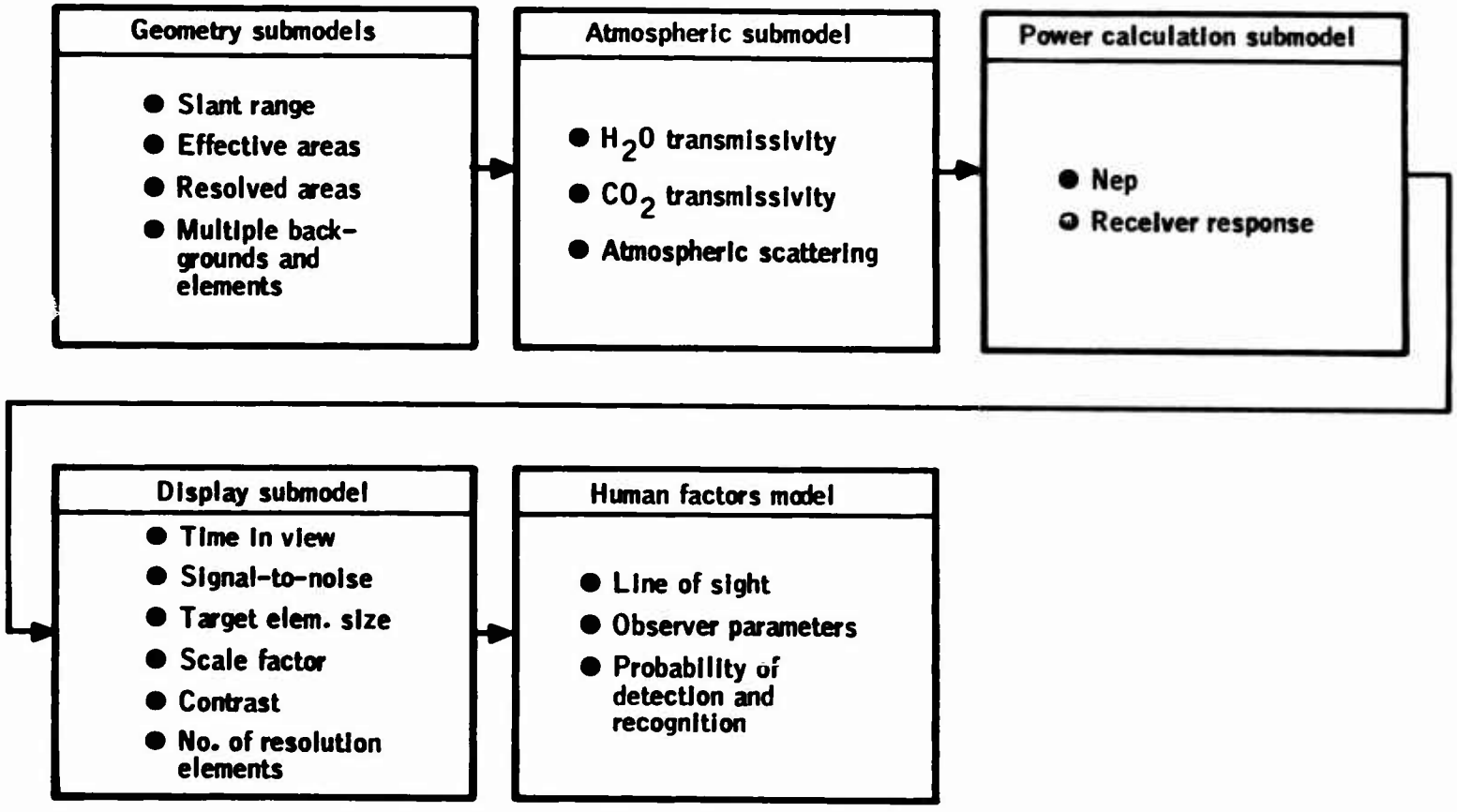

Figure B-4 -- Forward Looking Infrared Model Data Flow

LIBRARY DATA

This section contains and references the characteristic environment, target-element, and sensor subsystem data stored in the MARSAM library. The ten major categories of stored data, accompanied by a brief description of the types of data contained, are listed below:

- o Terrain Characteristics
  - Line-of-sight probability data for six terrain types
- o Weather Characteristics
  - Data applicable to the photographic, television, visual observer, and infrared sensor models for five weather conditions
  - Data applicable to the radar sensor models for ten weather conditions
- o Turbulence Characteristics
  - Data applicable to the photographic sensor models for three turbulence types
- o Target-Element Signatures
  - Dimensions, photo/visual reflectivity, emissivity, and radar cross-section for 81 target elements
- o Background Signatures
  - Photo/visual reflectivity, emissivity, and normalized radar cross-section for 15 backgrounds.
- o Sensor Subsystem Characteristics
  - Performance characteristics for:

    A forward-looking infrared subsystem

    A TV image orthicon subsystem

    A TV vidicon subsystem

APPENDIX C

SCATTERING OF ELECTROMAGNETIC WAVES

INTRODUCTION

Various sensors which could be used for an ILM depend on their operation on the reflective properties of the terrain in the microwave region. Many measurements of these properties have been made, however, the preponderance of the data is at incidence angles between 10 and 80 degrees. Since ILM sensors must operate with incidence angles from about 84 to 89 degrees, these data are not directly usable.

In an attempt to obtain usable data, a theoretical formulation of electromagnetic scattering was developed and programmed on a computer under the assumption that if the theoretical model corresponded to the measured data at those points where data was available, the model could be used to generate the needed data at higher incidence angles. The model used was a statistically rough surface using the Kirchoff approximation and at first appeared to give good correspondence. It was later noted that the formulation was missing a cosine of the incidence angle. After correcting the model, no set of parameters in the theoretical model could give correspondence with the measured data. Several explanations are possible for this. It has been pointed out that the source from which the model was obtained has an error in the dominant term of the equation at high incidence angles. Another problem is that only diffuse reflections are considered in the model with specular components

the scattering properties of the surfaces involved.

The technique selected to establish the scattering properties is to obtain a theoretical model of scattering which can be justified from physical principles. Any such model will have various parameters which can be adjusted to modify the scattering properties, so that it can represent various surfaces. The model will be applied to the measured backscattered data to establish the values of the parameters for the surface, and these parameters will then be used to generate angular relationships.

Definitions for Scattering Parameters

The most physical scattering parameter is the reflection coefficient. It is defined in terms of the field strengths at the reflecting interface as

$$R = \frac{E_R}{E_I} \qquad \text{(C-1)}$$

where R is the reflection coefficient
E_R is the reflected field
E_I is the incident field

While this is an adequate parameter for perfectly conducting, finite size, smooth targets, it is difficult to use.

For an area target, the concept of cross section is generalized to a dimensionless cross section per unit area, such that the radar range equation becomes:

$$P_r = \frac{P_t \lambda^2}{(4\pi)^3 r^4} \int_s \gamma G_t G_R \, dS \qquad \text{(C-3)}$$

where s is the reflecting surface

γ is the differential cross section per unit surface area.

G_t, G_R are the antenna gains in the direction of the differential area dS

This equation is often used in the form:

$$P_r = \frac{P_t G_t G_R \lambda^2}{(4\pi)^3 r^4} \int_s \gamma \, dS \qquad \text{(C-4)}$$

which assumes that the gain across the antenna beamwidth is constant and zero outside the beam. By examining this equation, it can be seen that for finite targets

$$\gamma = \frac{4 \pi A}{\lambda^2} R^2 \qquad \text{(C-5)}$$

where A is the target area

R is the reflection coefficient

λ is the wavelength.

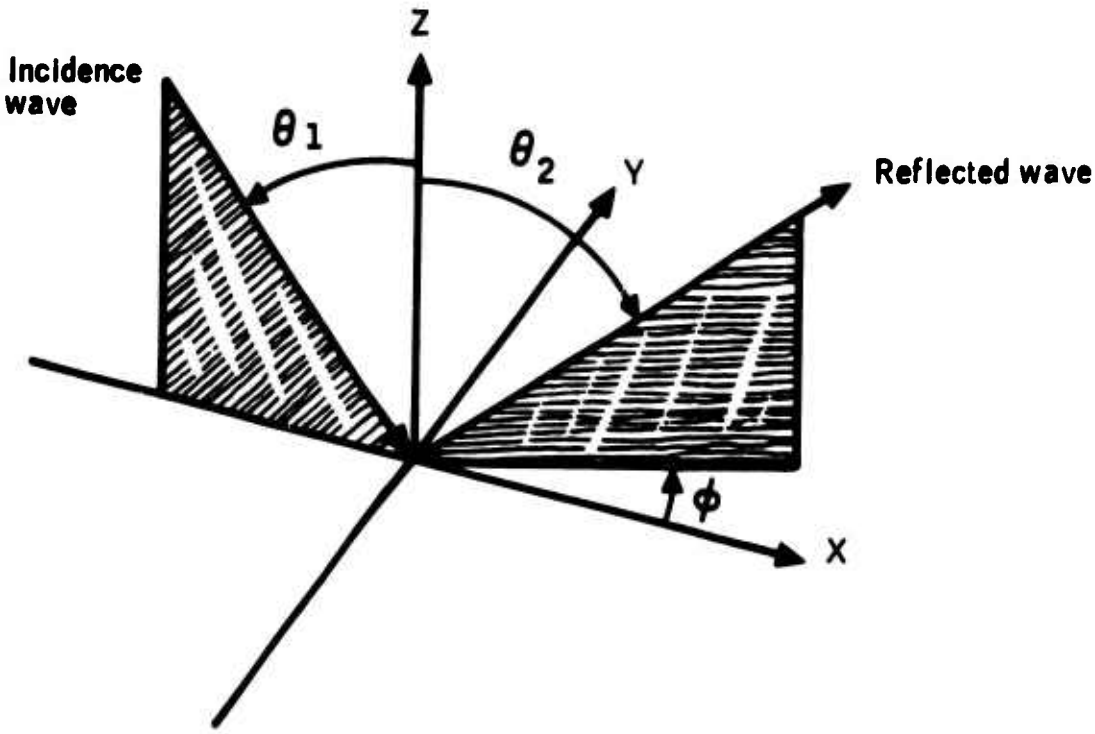

Figure C-1 -- Scattering Geometry

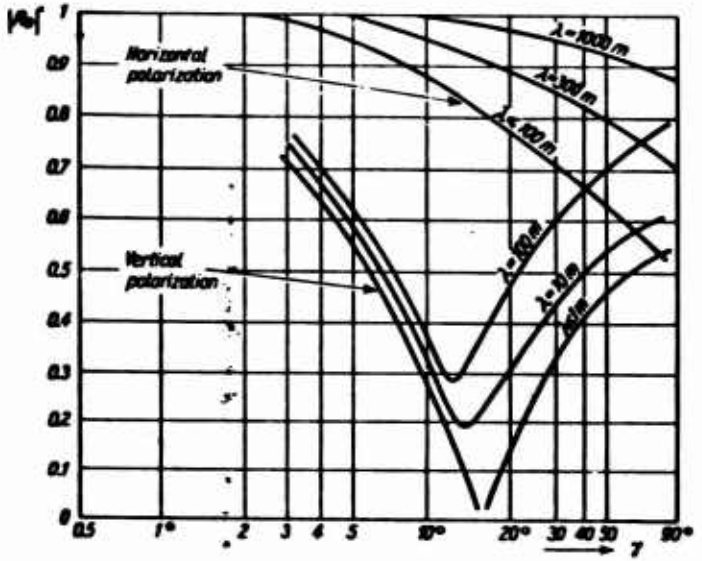

Reflection coefficient of a perfectly plane earth with $\varepsilon/\varepsilon_0 = 10$, $\sigma = 10^{-3}$ mho/m.

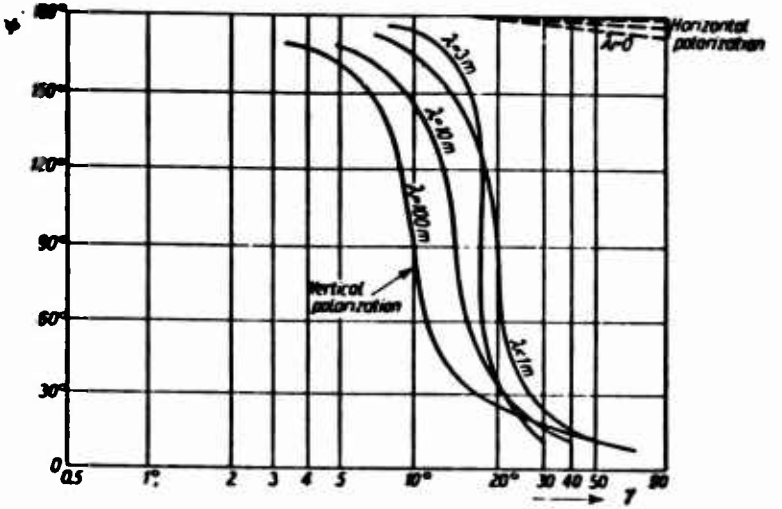

Phase Φ of the reflection coefficient of a perfectly plane earth. $\varepsilon/\varepsilon_0 = 10$, $\sigma = 10^{-3}$ mho/m.

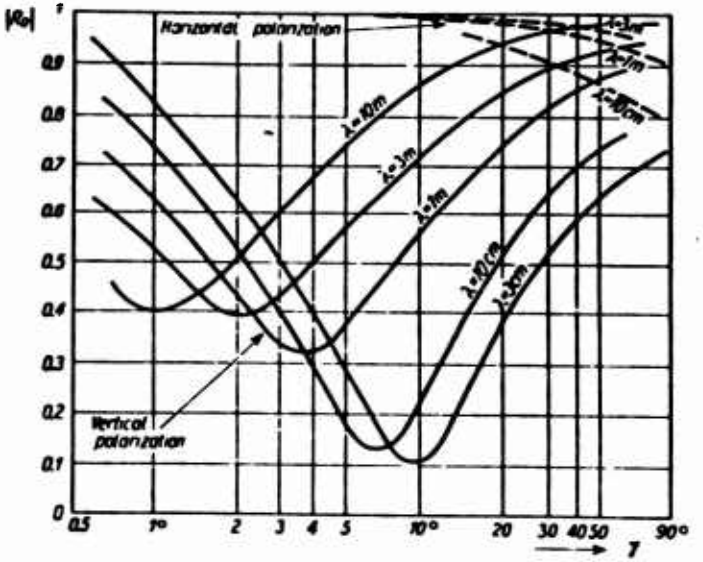

Reflection coefficient of a very smooth sea. $\varepsilon/\varepsilon_0 = 80$, $\sigma = 4$ mho/m.

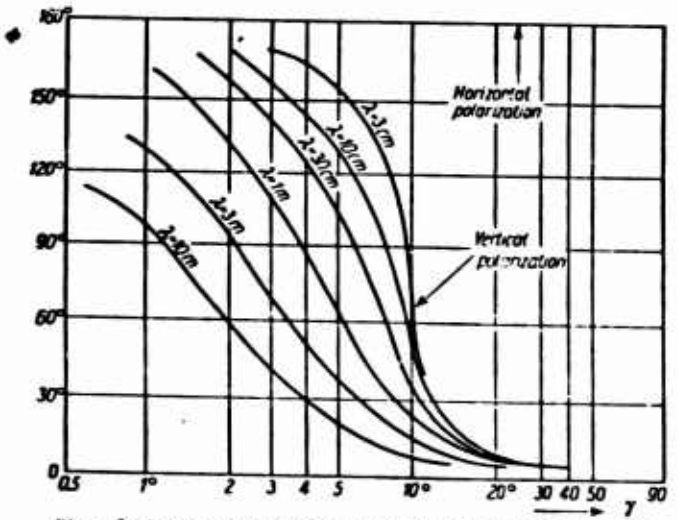

Phase Φ of the reflection coefficient of a very smooth sea. $\varepsilon/\varepsilon_0 = 80$, $\sigma = 4$ mho/m.

Figure C-2 -- Fresnel Reflection Coefficients

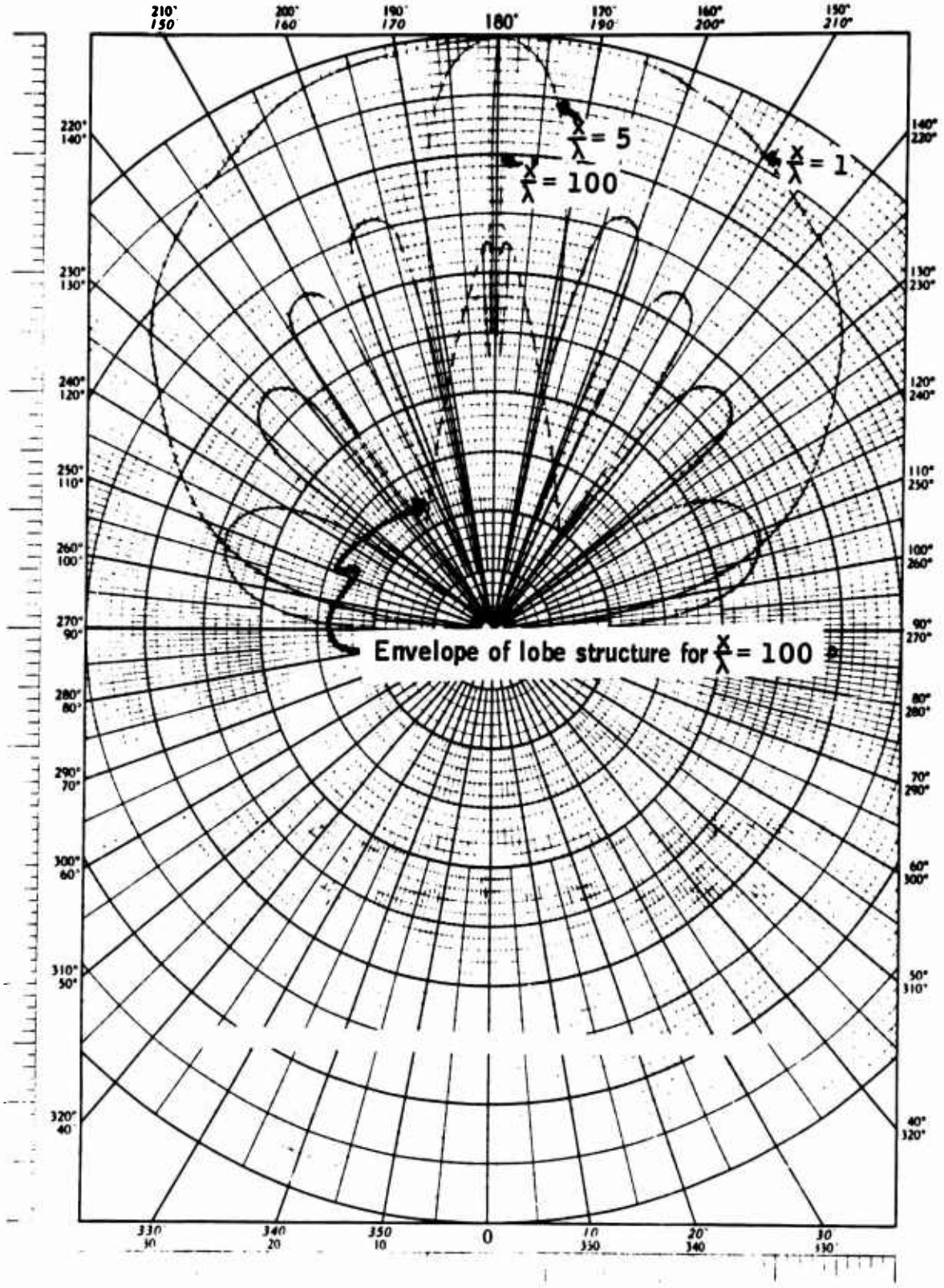

Figure C-3 -- Specular Scattering from a Smooth Finite Surface

K_1 is the propagation vector of the incident wave

K_2 is the propagation vector of the reflected wave

n is the unit normal to the surface

$p = K_1 + K_2$

For a finite surface area in cartesian coordinates,

$$E = \frac{jk \exp(jkr)}{4 \pi r} \int_S (a\rho'_x + c\,\rho'_y - b)\; e^{j\vec{v}\cdot\vec{r}}\; dS \qquad \text{(C-14)}$$

where $a = (1-F)\sin\theta_1 + (1+F)\sin\theta_2 \cos\phi$

$b = (1-F)\cos\theta_2 - (1-F)\cos\theta_1$

$c = (1+F)\sin\theta_2 \cos\phi$

$\rho(x,y)$ is the height of the surface at (x,y)

$$\rho'_x = \frac{d\rho}{dx}$$

Since the field due to a perfectly conducting area of the same size is

$$E = \frac{jkA \cos\theta_1 \exp(jkr)}{2\pi r} \qquad \text{(C-15)}$$

A reflection coefficient for the rough surface can be defined as

$$\rho = \frac{1}{2A\cos\theta_1} \int_S (a\rho'_x + C\,\rho'_y - b)\; e^{i\vec{v}\cdot\vec{r}}\, dS \qquad \text{(C-16)}$$

where $\vec{V} = \frac{2\pi}{\lambda}\left[(\sin\theta_1 - \sin\theta_2 \cos\phi)\,\vec{i} - \sin\theta_2 \sin\phi\,\vec{j} - (\cos\theta_1 + \cos\theta_2)\,\vec{k}\right]$

$\vec{i}, \vec{j}, \vec{k}$ is the unit vector triad

The integral in the expression for $\langle \rho\rho^* \rangle$ depends on $\langle e^{iv_t(\zeta - \zeta)} \rangle$, which is the characteristic function of the probability distribution of ζ. Therefore, to proceed further it is necessary to define this distribution. By the central limit theorem, it can be expected that the surface is Guassianaly distributed in height. Two correlation functions, corresponding to "peaky" and more smoothly bumpy surfaces will be investigated. The characteristic function for a gaussian surface is:

$$\langle e^{iv_z(\zeta - \zeta)} \rangle = \exp\left(-v_z^2 \sigma^2 (1 - C(\tau))\right) \qquad \text{(C-19)}$$

where σ^2 is the variance of surface height

$C(\tau)$ is the correlation coefficient

Slightly Rough Surfaces

If the surface is slightly rough in the sense that $V_z^2 \sigma^2 << 1$, then the power series for the exponential will converge rapidly enough that only the first term has significant contribution to reflection. In this case, the integral is readily evaluated yielding (Ref. C-1, C-4)

$$\langle \rho\rho^* \rangle = \frac{\pi |F|^2 \; V_z^2 \; \sigma^2 \; T^2}{A} \exp\left(-V_z^2 \sigma^2 - \frac{V_{xy}^2 T^2}{4}\right) \qquad \text{(C-20)}$$

if $C(\tau) = e^{-\tau^2/T^2}$

and

$$\langle \rho\rho^* \rangle = \frac{2\pi |F|^2 V_z^2 \sigma^2 T^2}{A \cos^2\theta (1 + V_{xy}^2 T^2)^{3/2}} \exp\left(-V_z^2 \sigma^2\right) \qquad \text{(C-21)}$$

if $C(\tau) = e^{-|\lambda|/T}$

Very Rough Surfaces

The other case which can be easily evaluated is the very rough surface, in the sense that $V_z \sigma^2 > > 1$. Since $V_z \sigma^2$ is very large, the characteristic function will have significant values only near $\tau=0$. Further, since the correlation function is by definition an even function, it's McLaurin series will contain only even powers. Since $C_j(0)=1$, this term contributes nothing to the expansion of the characteristic function about zero. Thus the only term of interest is the second derivative. Taking this expansion and performing the integration (ref C-4).

$$\langle \rho\rho^* \rangle = \frac{2\pi |F|^2}{A\, V_t^2 \sigma^2 C''(0)} \exp - V_{xy}^2 / 2V_z^2 \sigma^2 |C_j''(0)| \qquad \text{(C-24)}$$

for $C = e^{-t^2/T}$

$$\langle \rho\rho^* \rangle = \frac{2\pi F^2 V_z^2 \sigma^2}{T^2 A (V_z^2 \sigma^2 / T^2 + V_{xy}^2)^{3/2}} \qquad \text{(C-25)}$$

for $C = e^{-|\tau|/T}$

Converting to differential cross section,

$$\gamma = \frac{2 |F|^2 \left(\frac{V_z}{R}\right) \left(\frac{T}{\lambda}\right)^2 \exp\left[- \frac{\left(\frac{T}{\lambda}\right)^2 \left(\frac{V_{xy}}{R}\right)^2}{4 \left(\frac{\sigma}{\lambda}\right)^2 \left(\frac{V_z}{R}\right)^2} \right]}{\left(\frac{V_z}{R}\right)^4 \left(\frac{\sigma}{\lambda}\right)^2} \qquad \text{(C-26)}$$

for $C(z) = e^{-\tau^2/T^2}$

$$\gamma = \frac{4\pi |F|^2 \left(\frac{V_z}{R}\right)^2 \left(\frac{\sigma}{\lambda}\right)^2}{\frac{T}{\lambda}\left[(2\pi)^2 \left(\frac{V_z}{R}\right)^4 \left(\frac{\left(\frac{\sigma}{\lambda}\right)^2}{\frac{T}{\lambda}} \right)^2 + \left(\frac{V_{xy}}{R} \right)^2 \right]^{3/2}} \qquad \text{(C-27)}$$

for $C(\tau) = e^{-|\tau|/T}$

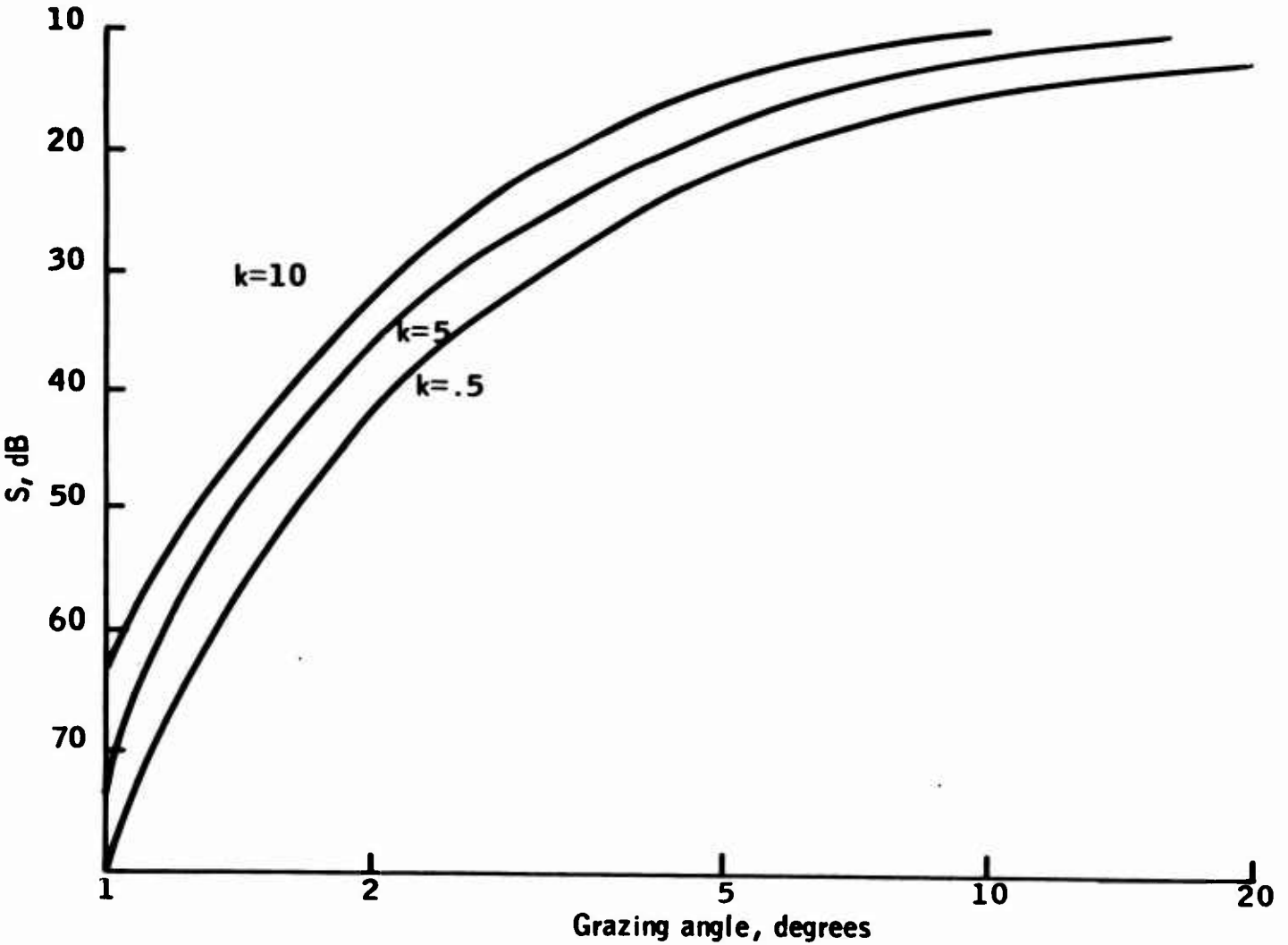

Figure C-4 -- The Shadowing Function

$$F_{HV} = \sin\phi \; \frac{\sin\theta_2 a_2 R_H(i) - \sin\theta_1 a_3 R_V(i)}{a_1 a_4} \qquad \text{(C-33)}$$

$$F_{VH} = \sin\phi \; \frac{\sin\theta_2 a_2 R_V(i) - \sin\theta_1 a_3 R_H(i)}{a_1 a_4} \qquad \text{(C-34)}$$

$$F_{HH} = \frac{-\sin\theta_1 \sin\theta_2 \sin^2\phi R_V(i) - a_2 a_3 R_H(i)}{a_1 a_4} \qquad \text{(C-35)}$$

where $a_1 = 1 + a_5$

$a_2 = \cos\theta_1 \sin\theta_2 + \sin\theta_1 \cos\theta_2 \cos\phi$

$a_3 = \sin\theta_1 \cos\theta_2 + \cos\theta_1 \sin\theta_2 \cos\phi$

$a_4 = \cos\theta_1 + \cos\theta_2$

$a_5 = \sin\theta_1 \sin\theta_2 \cos\phi - \cos\theta_1 \cos\theta_2$

$i = \arctan\sqrt{\frac{1+a_5}{1-a_5}}$

F_{JK} is the local Fresnel coefficient for J polarized transmission and K polarized reception.

Since this set of equations defines a scattering matrix, the reflection for arbitrary polarizations can be derived from it. In particular, for the circular polarizations.

$$F_{LR} = \frac{F_{HH} + F_{VV} + j\,(F_{HV} - F_{VH})}{2} \qquad \text{(C-36)}$$

$$F_{RR} = \frac{F_{HH} - F_{VV} + j\,(F_{HV} + F_{VH})}{2} \qquad \text{(C-37)}$$

$$F_{RL} = \frac{F_{HH} + F_{VV} - j\,(F_{HV} - F_{VH})}{2} \qquad \text{(C-38)}$$

$$F_{LL} = \frac{F_{HH} - F_{VV} - j\,(F_{HV} + F_{VH})}{2} \qquad \text{(C-39)}$$

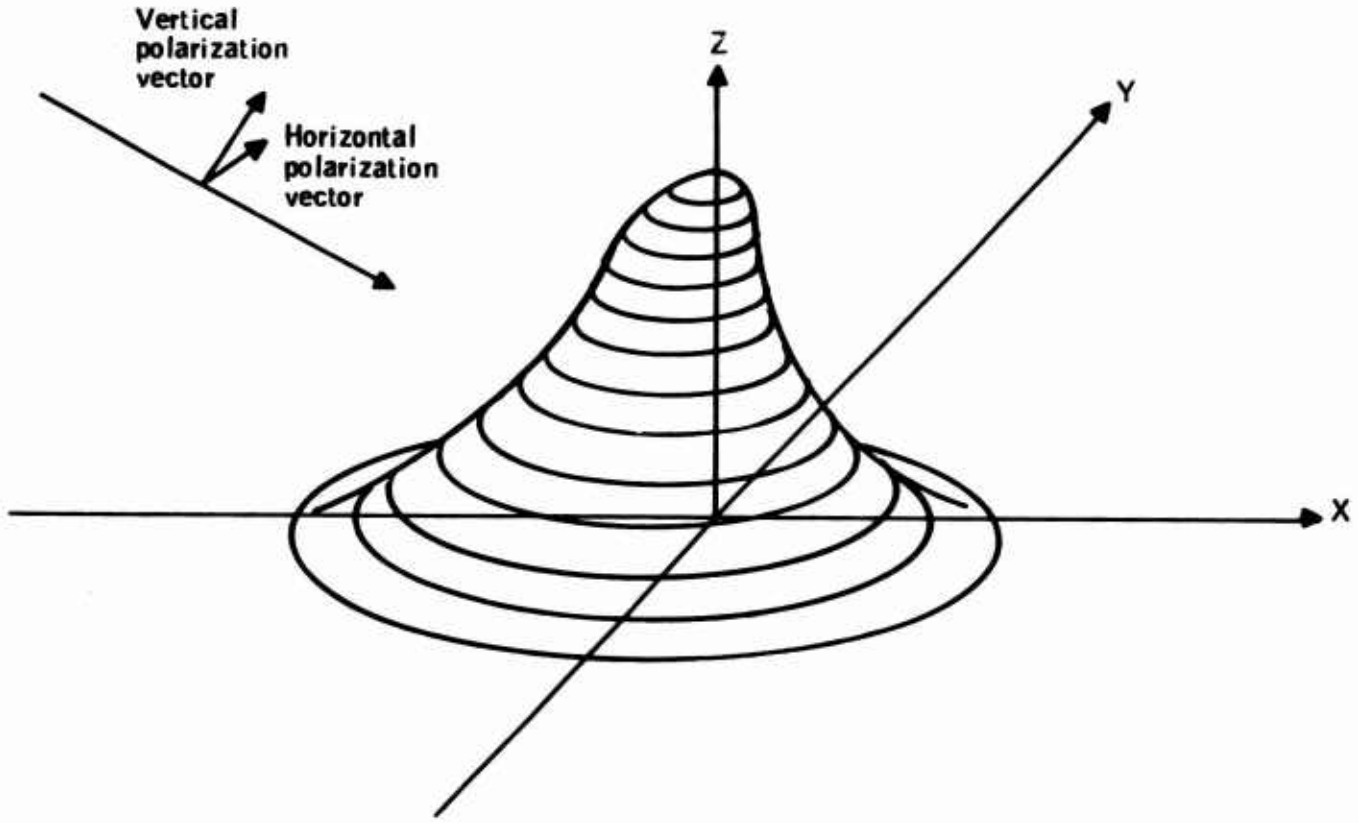

Figure C-5 -- Isotrophic Roughness

A main program, used to test the subroutine and establish surface parameter values has also been written. The test program obtains back-scattering cross sections from 10 to 80 degrees, and plots these cross sections along with a set of values which are input. By examining the resultant plot, it can be immediately determined how well the theoretical results match the measured data.

The name of the test program is TSTSCAT. The program reads in from the teletype values for the constant (measured) plot, scale roughness, scale slope, and permittivity. Polarization and correlation are changed by modifying the program. The call to STSCAT is made with continuation lines to enable modifying IPOL and ICOR with literals. Line 180 is IPOL, line 190 is ICOR. Thus, to enter a value of IPOL, the following program modification would be made

180 &[IPOL] ,

where [IPOL] is the value of IPOL, to change correlation, the equivalent modification is

190 & [ICOR] ,

A listing of the entire program, including the test drive program and the subroutine STSCAT follows:

```
230      RESULT(I)=SIG
240 10 ANGLE(I)=10*I
250      PRINT 260,SLP
260 260FORMAT("SLOPE=",F6.2)
270      PRINT 20,(ANGLE(I),I=1,10)
280      PRINT 30,(RESULT(I),I=1,10)
281      PRINT 282
282 282FORMAT(//)
290 15 CONTINUE
300 50 CONTINUE
305      PRINT 306
306 306FORMAT("PLOT ")
307      READ 380,REP
308      IF(REP.NE.YES) GO TO 338
310 20 FORMAT(10HINCIDENCE ,10F6.2)
320 30 FORMAT(10HCROSS SECT,10F6.2)
321      NMPT=2
322      YMAX=-10
323      YMIN=-50
324      CALL PLOT(XPLT,YPLT,YMAX,YMIN,NMPT,1,36)
325      KPLT=0
326      LPLT=1
327      DO 337 JPLT=1,36
328      XPLT=8.2*JPLT
329      LPLT1=LPLT+1
330      YPLT(1)=KPLT/5.0*(RESULT(LPLT1)-RESULT(LPLT))+RESULT(LPLT)
331      YPLT(2)=KPLT/5.0*(INGAM(LPLT1)-INGAM(LPLT))+INGAM(LPLT)
332      CALL PLOT(XPLT,YPLT,YMAX,YMIN,NMPT,0,36)
333      KPLT=KPLT+1
334      IF(KPLT.LT.5)GO TO 337
335      KPLT=KPLT-5
336      LPLT=LPLT+1
337 337CONTINUE
338 338PRINT 370
340      READ 380,REP
350      IF(REP.EQ.YES)GO TO 40
361      PRINT 364
362      READ 380,REP
363      IF(REP.EQ.YES)GO TO 31
364 364FORMAT("ANOTHER ARRAY",)
365 370 FORMAT("ANOTHER CASE")
370 380FORMAT(A3)
380                                    STOP
390                                    END
1010 SUBROUTINE STSCAT(AINC,AREFL,AOAZ,PRMTIV,IPOL,ICOR,ROUGH,SLOPE,GAMDB)
1020     COMPLEX PRMTIV,BVV,BVH,BHV,BHH,RVERT,RHORZ,BETA,BCONJ,CTEMP
1030     SNINC=SIN(AINC)
1040     SNREF=SIN(AREFL)
1050     SNOAZ=SIN(AOAZ)
1060     CSINC=COS(AINC)
1070     CSREF=COS(AREFL)
1080     CSOAZ=COS(AOAZ)
1082   TEMP1=AINC-AREFL
1083     IF(TEMP1.LT..00001)GO TO 430
1090     A5=CSINC*CSREF-SNINC*SNREF*CSOAZ
```

```
      GAMMA=3.1170909E3*BETA*(ROUGH*SLOPE)**2*EXP(-39.478417*(ROUGH*(
     &        CSINC+CSREF))**2)/(TEMP1*SQRT(TEMP1))
       K=SLOPE/(1.414*ROUGH)
  670 IF(CSINC.GT.CSREF)GO TO 750
      TEMP1=ABS(SNREF/CSREF)
      IF(K/TEMP1.LT.1)GO TO 730
      TEMP2=EXP(-(K/TEMP1)**2)
      SHADR=EXP(-TEMP1**2*TEMP2/(3.5549*K))
      GO TO 760
  730 SHADR=EXP(-(TEMP1-K)/3.5549)
      GO TO 760
  750 SHADR=1
  760 TEMP1=ABS(SNINC/CSINC)
      IF(K/TEMP1.LT.1)GO TO 810
      TEMP2=EXP(-(K/TEMP1)**2)
      SHADI=EXP(-TEMP1**2*TEMP2/(3.55490707*K))
      GO TO 820
  810 SHADI=EXP(-(TEMP1-K)/3.5449077)
  820 GAMMA=GAMMA*SHADR*SHADI
  830 IF(GAMMA.GT.0)GO TO 870
      PRINT 880,GAMMA
  850 GAMDB=99.99
      GO TO 890
  870 GAMDB=10*ALOG10(GAMMA)
  880 FORMAT(11HGAMMA ERROR,F6.2)
  890 RETURN
      END
```

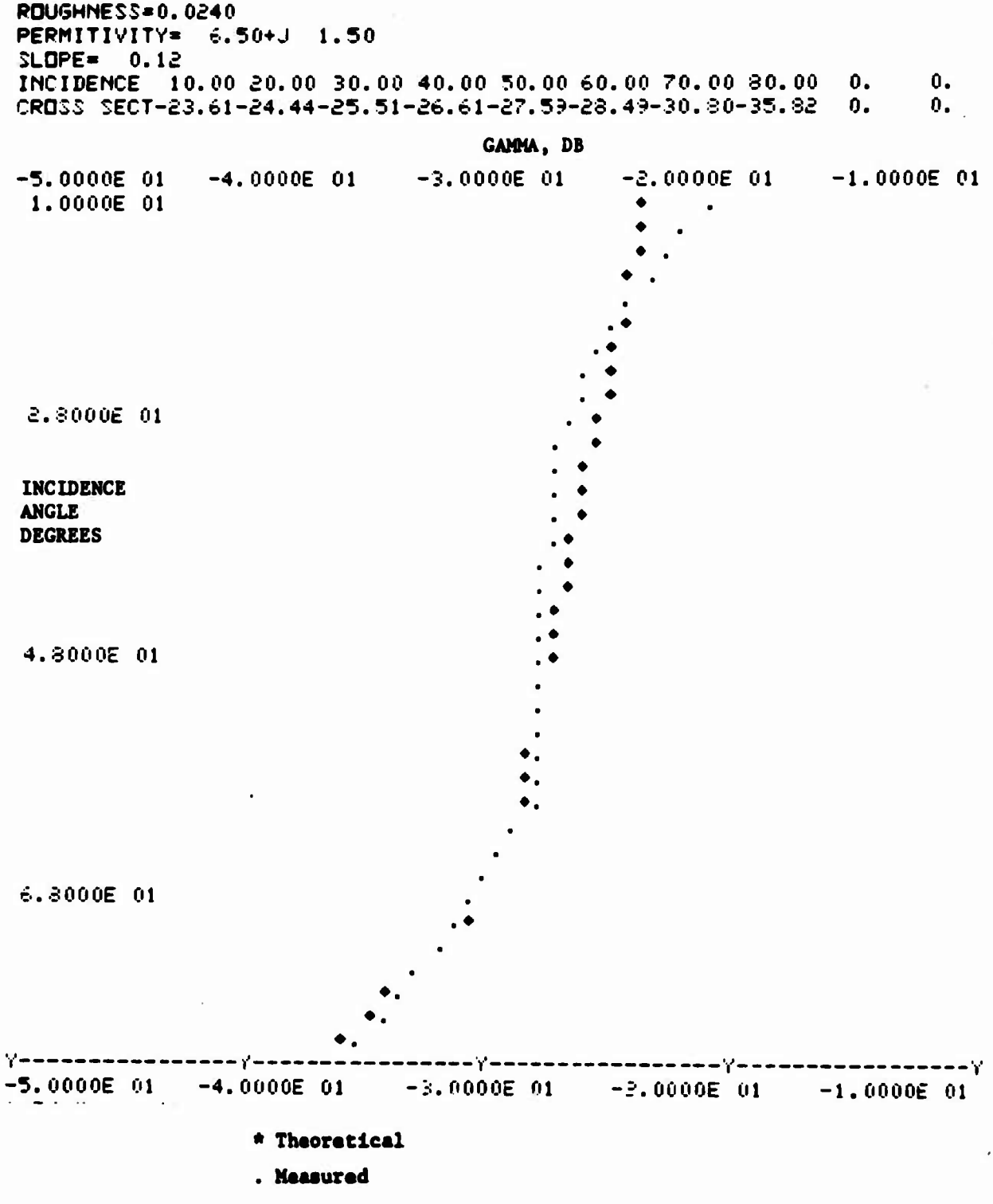

Figure C-6--Best Match for Backscatter from Concrete at X-band, vertical polarization

Taking the surface parameters which yield the best data at X-band and directly scaling them to K-band yield figures C-8 and C-9. These figures show a relatively good match between the theoretical prediction and the measured data. A few other values for the slope and roughness parameters have been attempted, with poorer results.

Figure C-10 shows the result of a computation for vertical polarized X-band backscatter off an asphalt surface. Again, the only significant deviation between theory and measurement is at angles which could have significant specular contributions.

APPLICATION OF SCATTERING MODELS TO ILM

Information on the scattering properties of natural surface is required in several areas of the ILM sensor analysis. Scattering data provides a means for

- o Differential cross section estimation
- o Multipath environment definition
- o Mutual interference analysis

Extension of Cross Section Data

The most obvious usage of scattering models is to extrapolate available radar cross section data. Nearly all of the measured cross section data available is for incidence angles between 10 and 80 degrees. For the ILM program, 84 to 88 degrees are typical incidence angles. Thus at incidence angles of interest, very little data is available. Further, the beamwidth

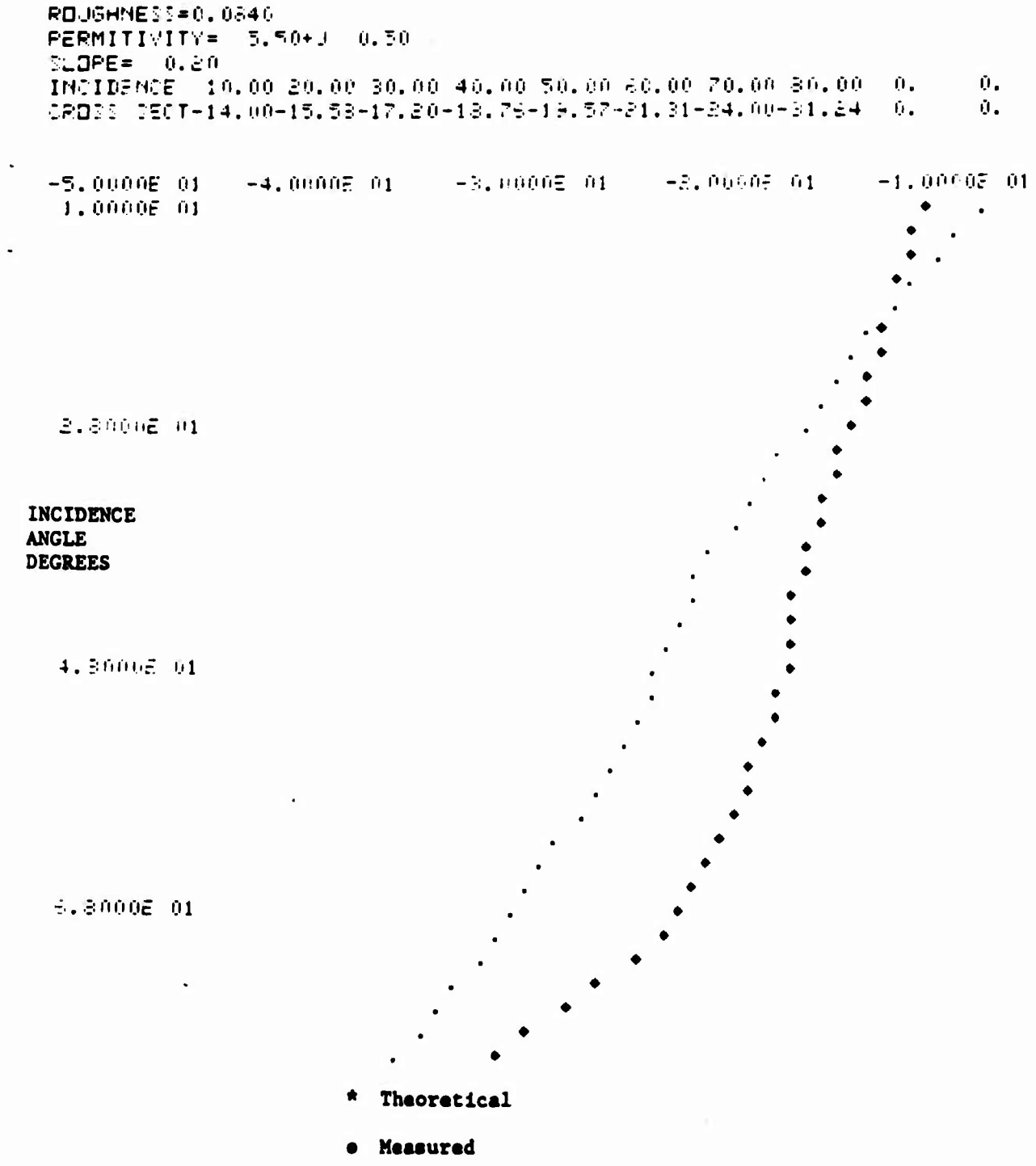

Figure C-9-- Backscatter from concrete at K_a band, horizontal polarization

and sidelobe levels of the measuring antenna are not normally known. At high incidence angles where the differential cross section is relatively high and changing slowly with angle these items are fairly unimportant. However, at low grazing angles, the cross section is low and varies rapidly with angle. Therefore, antennas of different beamwidth (or systems with diffeerent pulse width for a pulse measuring system) can have large discrepancies when measuring the same surface, since the major power contribution may come from slightly different angles. Also, when the cross section is very low and the measuring system uses a CW technique, significant error contributions can be made by energy entering the sidelobes. Thus, even that data which is available at these low grazing angles is of questionable validity. Since a computer program is available which provides cross section data in good agreement with the high angle measured data, which is in some sense mathematically reasonable, and which is intuitively correct, the outputs from this program can be used with some confidence.

The same caveat applies to using the theoretical results as was mentioned in criticizing the measurements. The cross section is changing rapidly with incidence angle, and thus some gain function must be included in the integration of the radar range equation

$$P_r = \frac{P_t \lambda^2}{(4\pi)^3} \int_S \frac{G_t G_R \gamma}{R^4} \, dS \qquad \text{(C-41)}$$

In this model, all significant contributions to the received energy come from areas where $\xi_{xy}<\beta_o$. By extending this approximation to all models the glistening surface, i.e., that area having significant contribution to the diffuse multipath signal, may be defined.

It can be derived geometrically that if the area is not limited by the antenna patterns of the transmitting and receiving antennas, the glistening surface is approximately a trapazoid with sides defined by (ref. C-1).

$$\beta = \beta_o$$

and ends defined by

$$d_i = h_i \cot 2\beta_o \qquad i=r,t$$

where d_i is the distance to the start of the glistening surface from the ith antenna

as shown in Figure C-11.

Limiting the area of integration to this surface, the mean value of received diffuse multipath power is given by the bistatic radar range equation:

$$P_r = \frac{P_t \lambda^2}{(4\pi)^3} \int_S \frac{\gamma\,(\theta_1,\theta_2,\phi)\; G_t(\theta_1-\theta_t, \frac{\phi}{2})\; G_R\,(\theta_2-\theta_R, \frac{\phi}{2})\;\; dS}{R_1^2 R_2^2} \qquad (C\text{-}43)$$

where θ_t is the transmitting depression angle

θ_r is the receiving elevation angle

Many analyses (ref C-1 chapter 7 for example) have shown that the distribution of this power is approximately uniform in phase and Rayleigh in power. Since any other assumption yields an extremely complex expression depending on surface parameters, polarization, etc., the Rayleigh distribution will be assumed here. Thus the diffuse multipath appears at the receiver as an additive noise term, which provides an upper limit on the signal to noise ratio.

Since the width of the glistening surface is very narrow, the azimuth antenna gain variation and change in cross section can be approximated as a constant. The width of the glistening surface is:

$$\omega = \left[h_2 + {}_{\ell} h_2 \tan\theta_2 (h_1 - h_2) \right] \tan \beta_o$$

where h_1 is the height of the transmitting antenna

h_2 is the height of the receiving antenna

ℓ is the ground range from the transmitter to the receiver

The total diffuse multipath power is then:

$$P_r = \frac{P_t \lambda^2}{(4\pi)^3} \int_{h_2 \cot\beta_o}^{h_1 \cot\beta_o} \frac{\gamma \left(\tan^{-1}\left(\frac{\ell - r}{h_1}\right), \tan^{-1}\left(\frac{r}{h_2}\right), 0\right) G_t \left(\tan^{-1}\left(\frac{h_1}{\ell - r}\right) - \theta_t, 0\right)}{(\ell - r)^2 r^2}$$

$$\frac{G_r \left(\tan^{-1}\left(\frac{h_2}{r}\right) - \theta_r, 0\right) (r h_1 + (\ell - r) h_2) \; 2 \tan \beta_o}{} \, dr$$

REFERENCES

1. Beckmann and Spizzichino, The Scattering of Electro Magnetic Waves from Rough Surfaces, MacMillan, 1963.

2. Semenov, Scattering of Electromagnetic Waves from Restricted Portions of Rough Surfaces with Finite Conductivity, Radiotekhnika i Electronica V, 110, 1965, p. 1952.

3. Barrick, D. E., Rough Surface Scattering Based on the Specular Point Theory, AP16 1968, P449.

4. Beckmann, Scattering by Composite Rough Surfaces, Proc. IEEE, Vol. 53 No. 8, August 1965, p. 1012.

5. Beckmann, Shadowing by Random Rough Surfaces, AP13, May 1965, p. 384.

6. Ruck, Barrick, Stuart, and Krichbaum, Radar Cross Section Handbook, Vol. 2, Plenum Press, 1970.

7. Mitzner, K.: Change in Polarization on Reflection from a Tilted Plane, Radio Science, Vol. 1, 1966, pg. 27.

APPENDIX D
ATMOSPHERIC ATTENUATION OF MICROWAVES

GASEOUS ABSORPTION

The absorption of microwave energy by atmospheric gases is due to cyclotron resonance of the molecules of the constituent gases. In the frequency range of microwave sensors, the absorption is due to the 1.35 cm resonance of water vapor and a series of resonances of oxygen centered about .5 cm.

The general theory of gaseous absorption of microwaves has been formulated by VanVleck (Reference D-1) and the constants in the formula measured by Birnbaum and Maryott (Reference D-2), Artman and Gordon (Reference D-3), and Becker and Autler (Reference D-4).

The absorption by oxygen is given by:

$$\alpha_o = \frac{34}{\lambda^2} P \left(\frac{293}{T}\right)^2 \left[\frac{\Delta V_1}{1/\lambda^2 + \Delta V_1^2} + \frac{\Delta V_2}{(2+1/\lambda)^2+\Delta V_2^2} + \frac{\Delta V_2}{(2-1/\lambda)^2+\Delta V_2^2}\right] \quad \text{(D-1)}$$

where

α_o is the attenuation in dB/Km

λ is the wavelength in cm

P is the pressure in atmospheres

T is the temperature in degrees Kelvin

$\Delta V_1 = .018\ P\ \left(\frac{293}{T}\right)^{3/4}$

$\Delta V_2 = .049\ P\ \left(\frac{300}{T}\right)^{3/4}$

where

$\alpha_d \approx \frac{15.8P}{T_o^2}$ is the ground level dry absorption coefficient

h is the altitude (Km)

k is the temperature/lapse rate

T_o is the ground level temperature (°K)

$\alpha_\omega \approx (24 - \frac{T_o}{20}) \frac{Pw \times 10^{-3}}{101.3}$ is the ground level wet absorption coefficient

P is the atmospheric pressure (KPa)

W is the absolute humidity (g/m^3)

This model is useful because of its analytical tractability. Since the maximum gaseous attenuation of interest is less than 5 dB, any errors caused by the use of this formula will be insignificant.

ATTENUATION BY CLOUDS OR FOG

Attenuation of microwave by clouds or fog is of a considerably different nature than that due to either rain or water vapor. This is due to the scattering characteristics of the very small (<.01 cm) diameter drops. Fog attenuation was derived by Gunn and East (Reference D-5) with the results shown in Table D-1. Attenuation at frequencies below X band are not significant over the path lengths considered, for example at 3 GHz with a 30 m visibility, it requires a 50 Km path to obtain 1 dB of path attenuation.

The data in Table D-1 is presented in terms of $dB/Km/g/m^3$ which requires knowledge of the amount of condensed water. Based on attenuation measure-

Table D-2. Assumed Water Content of Fog

RVR, ft	g/m^3 of Water
1,200	.065
700	.14
150	1.1
0	4.0

ATTENUATION BY RAIN

The attenuation of microwaves by rain is the most significant and simultaneously the least predictable of all atmospheric degradations. The theoretical foundation for predicting rain attenuation is the paper of Ryde and Ryde (Reference D-6), which assumed a particular distribution of water drop sizes and derived expression for attenuation based on Mie scattering. The resultant attenuation values can be quite closely approximated by a function of the form

$$A = kaR^b \qquad \text{(D-5)}$$

where

A is the specific attenuation (dB/Km)

a is a function of frequency

k is a function of temperature and frequency

R is the rainfall rate (mm/hr)

b is a function of frequency

The only attenuation measurements which differed from Rydes theory via the reflectivity approximation were measurement where there was evidence of hail or snow mixed in the rain. In these cases, the attenuation was significantly less than it would be for pure rain, as theory predicts.

Therefore, it appears that inconsistancies in measured data are due more to inaccuracies in measuring the spatial and temporal variations of the rain than to any basic fault in Rydes theory. Medhurst's minimum and maximum limits are not reasonable for radar performance calculation, since it is highly improbably that any rain shower would consist of uniformly sized drops, pathologically sized to provide the highest or lowest possible attenuation. Any arbitrary variance in attenuation would be as mathematically viable as Medhurst's minimum and maximum.

ATTENUATION BY ICE AND SNOW

Solid water can be present in the atmosphere in several forms: ice fog or cloud, hail, or snow. Because of the different dielectric constants of solid water, its attenuation is generally insignificant. However, if the solid water is coated with a layer of liquid water, it's attenuation can be as great or even greater than the attenuation of the equivalent liquid water particle.

Therefore, the specific attenuation of ice fog or ice clouds will be considered to be zero, as will the attenuation of hail or snow if the air temperature surrounding the hail or snow is below 0°C. If the

The vertical profiles for the various cases is shown in Figure D-1.

Based on the weather cases defined above, specific attenuation profiles for C, X, Ku and Ka bands have been computed as shown in Tables D-4 through D-10. Gaseous absorption was computed using the VanVleck equations. Rain, cloud, and fog attenuations were computed by interpolating values from Tables D-1 through D-3.

Since the fog for weather case 2 is only 60m thick, it can be assumed to be at constant temperature. Therefore, Table D-5 is only the gaseous attenuation. The specific attenuation of fog must be added in the first 60m to compute the total specific attenuation. Values of fog attenuation for weather case 2 are given in Table D-11 on page D-15.

Table D-4-- SPECIFIC ATTENUATION DB/KM, ILM WEATHER CASE 1

ALTITUDE KILOMETERS	C BAND 6 GHZ	X-BAND 9 GHZ	KU BAND 15 GHZ	KA BAND 35 GHZ	TEMP °K
0.00	0.9000E-01	0.2775E 00	0.8412E 00	0.3196E 01	295.0000
0.10	0.9043E-01	0.2785E 00	0.8430E 00	0.3199E 01	294.3500
0.20	0.9097E-01	0.2796E 00	0.8449E 00	0.3201E 01	293.7000
0.30	0.9131E-01	0.2807E 00	0.8469E 00	0.3204E 01	293.0500
0.40	0.9176E-01	0.2817E 00	0.8488E 00	0.3207E 01	292.4000
0.50	0.1016E 00	0.3115E 00	0.9091E 00	0.3475E 01	291.7500
0.60	0.1022E 00	0.3132E 00	0.9126E 00	0.3481E 01	291.0908
0.70	0.1019E 00	0.3117E 00	0.9086E 00	0.3468E 01	290.4316
0.80	0.1015E 00	0.3097E 00	0.9035E 00	0.3453E 01	289.7725
0.90	0.1010E 00	0.3078E 00	0.8984E 00	0.3438E 01	289.1133
1.00	0.1005E 00	0.3059E 00	0.8933E 00	0.3424E 01	288.4541
1.10	0.1001E 00	0.3039E 00	0.8882E 00	0.3409E 01	287.7949
1.20	0.9963E-01	0.3019E 00	0.8832E 00	0.3394E 01	287.1357
1.30	0.9918E-01	0.3000E 00	0.8782E 00	0.3380E 01	286.4766
1.40	0.9874E-01	0.2981E 00	0.8732E 00	0.3365E 01	285.8174
1.50	0.9830E-01	0.2962E 00	0.8682E 00	0.3351E 01	285.1582
1.60	0.9789E-01	0.2944E 00	0.8638E 00	0.3338E 01	284.5512
1.70	0.9750E-01	0.2928E 00	0.8596E 00	0.3326E 01	283.9606
1.80	0.9711E-01	0.2911E 00	0.8554E 00	0.3314E 01	283.3701
1.90	0.9680E-01	0.2894E 00	0.8513E 00	0.3302E 01	282.7795
2.00	0.9659E-01	0.2876E 00	0.8475E 00	0.3290E 01	282.1890
3.00	0.9470E-01	0.2699E 00	0.8100E 00	0.3172E 01	276.2835
4.00	0.9492E-01	0.2626E 00	0.7938E 00	0.3119E 01	270.9718
5.00	0.9827E-01	0.2693E 00	0.8045E 00	0.3147E 01	265.5238
6.00	0.2038E-01	0.5701E-01	0.1258E 00	0.4496E 00	259.5714
7.00	0.1654E-01	0.4633E-01	0.1021E 00	0.3651E 00	253.0682
8.00	0.3352E-02	0.8336E-02	0.1778E-01	0.6311E-01	246.2572
9.00	0.2663E-02	0.6629E-02	0.1410E-01	0.5007E-01	239.0394

Table D-6 -- SPECIFIC ATTENUATION DB/KM, ILM WEATHER CASE 3.1

ALTITUDE KILOMETERS	C BAND 6 GHZ	X-BAND 9 GHZ	KU BAND 15 GHZ	KA BAND 35 GHZ	TEMP °K
0.00	0.9346E-02	0.1521E-01	0.3165E-01	0.1077E 00	282.7000
0.10	0.9185E-02	0.1503E-01	0.3126E-01	0.1064E 00	282.0300
0.20	0.9030E-02	0.1485E-01	0.3088E-01	0.1052E 00	281.4600
0.30	0.8879E-02	0.1468E-01	0.3051E-01	0.1040E 00	280.8400
0.40	0.8733E-02	0.1452E-01	0.3016E-01	0.1028E 00	280.2200
0.50	0.1234E-01	0.2551E-01	0.5410E-01	0.1919E 00	279.6000
0.60	0.1233E-01	0.2567E-01	0.5457E-01	0.1935E 00	278.8578
0.70	0.1232E-01	0.2584E-01	0.5506E-01	0.1951E 00	278.1156
0.80	0.1232E-01	0.2602E-01	0.5556E-01	0.1968E 00	277.3734
0.90	0.1232E-01	0.2620E-01	0.5607E-01	0.1985E 00	276.6312
1.00	0.1233E-01	0.2639E-01	0.5659E-01	0.2002E 00	275.8891
1.10	0.1234E-01	0.2658E-01	0.5712E-01	0.2020E 00	275.1469
1.20	0.1236E-01	0.2678E-01	0.5768E-01	0.2038E 00	274.4047
1.30	0.1237E-01	0.2698E-01	0.5823E-01	0.2057E 00	273.6625
1.40	0.1240E-01	0.2721E-01	0.5881E-01	0.2076E 00	272.9203
1.50	0.1245E-01	0.2756E-01	0.5948E-01	0.2100E 00	272.1781
1.60	0.1241E-01	0.2769E-01	0.5975E-01	0.2110E 00	271.7507
1.70	0.1235E-01	0.2775E-01	0.5991E-01	0.2116E 00	271.4226
1.80	0.1229E-01	0.2781E-01	0.6007E-01	0.2122E 00	271.0945
1.90	0.1223E-01	0.2789E-01	0.6024E-01	0.2129E 00	270.7664
2.00	0.1218E-01	0.2796E-01	0.6042E-01	0.2136E 00	270.4383
3.00	0.1187E-01	0.2893E-01	0.6263E-01	0.2219E 00	267.1575
4.00	0.1133E-01	0.2881E-01	0.6253E-01	0.2218E 00	264.2066
5.00	0.1969E-02	0.2485E-02	0.4184E-02	0.1332E-01	258.1250
6.00	0.1671E-02	0.2031E-02	0.2924E-02	0.9179E-02	242.5000
7.00	0.1328E-02	0.1616E-02	0.2270E-02	0.7149E-02	234.7717
8.00	0.1051E-02	0.1288E-02	0.1803E-02	0.5715E-02	227.8819
9.00	0.8357E-03	0.1034E-02	0.1457E-02	0.4654E-02	220.9921

Table D-10 -- SPECIFIC ATTENUATION DB/KM, ILM WEATHER CASE 4

ALTITUDE KILOMETERS	C BAND 6 GHZ	X-BAND 9 GHZ	KU BAND 15 GHZ	KA BAND 35 GHZ	TEMP °K
0.00	0.8527E-02	0.1019E-01	0.1506E-01	0.4630E-01	268.0000
0.10	0.8314E-02	0.9928E-02	0.1465E-01	0.4504E-01	267.3400
0.20	0.8107E-02	0.9677E-02	0.1425E-01	0.4380E-01	266.6800
0.30	0.7905E-02	0.9431E-02	0.1386E-01	0.4260E-01	266.0200
0.40	0.7709E-02	0.9192E-02	0.1348E-01	0.4142E-01	265.3600
0.50	0.7517E-02	0.8958E-02	0.1311E-01	0.4027E-01	264.7000
0.60	0.7308E-02	0.8705E-02	0.1271E-01	0.3905E-01	264.3387
0.70	0.7104E-02	0.8459E-02	0.1233E-01	0.3786E-01	263.9773
0.80	0.6906E-02	0.8220E-02	0.1195E-01	0.3670E-01	263.6160
0.90	0.6714E-02	0.7988E-02	0.1158E-01	0.3556E-01	263.2547
1.00	0.6527E-02	0.7761E-02	0.1123E-01	0.3446E-01	262.8934
1.10	0.6345E-02	0.7541E-02	0.1088E-01	0.3339E-01	262.5320
1.20	0.6168E-02	0.7327E-02	0.1054E-01	0.3234E-01	262.1707
1.30	0.5996E-02	0.7119E-02	0.1021E-01	0.3132E-01	261.8094
1.40	0.5829E-02	0.6917E-02	0.9885E-02	0.3032E-01	261.4480
1.50	0.5666E-02	0.6720E-02	0.9571E-02	0.2935E-01	261.0867
1.60	0.5495E-02	0.6527E-02	0.9344E-02	0.2869E-01	261.0499
1.70	0.5324E-02	0.6339E-02	0.9149E-02	0.2814E-01	261.1155
1.80	0.5159E-02	0.6157E-02	0.8960E-02	0.2761E-01	261.1811
1.90	0.4999E-02	0.5982E-02	0.8777E-02	0.2709E-01	261.2467
2.00	0.4844E-02	0.5811E-02	0.8599E-02	0.2659E-01	261.3123
3.00	0.3542E-02	0.4374E-02	0.7089E-02	0.2228E-01	261.9685
4.00	0.2709E-02	0.3332E-02	0.5237E-02	0.1646E-01	256.9718
5.00	0.2095E-02	0.2557E-02	0.3825E-02	0.1200E-01	250.9702
6.00	0.1664E-02	0.2019E-02	0.2882E-02	0.9039E-02	242.7857
7.00	0.1318E-02	0.1604E-02	0.2258E-02	0.7114E-02	235.4751
8.00	0.1044E-02	0.1279E-02	0.1791E-02	0.5678E-02	228.5066
9.00	0.8262E-03	0.1023E-02	0.1442E-02	0.4609E-02	221.9449

Table D-11. Specific Attenuation of Fog for Weather Case 2. (Db/km)

Subcase	RVR	C Band	X Band	Ku Band	Ka Band
2.1	1200 ft	.0015	.0047	.010	.038
2.2	700 ft	.0033	.010	.022	.082
2.3	150 ft	.026	.080	.171	.645
2.4	0 ft	.096	.292	.620	2.34

APPENDIX E

RADIOMETRY COMPUTER PROGRAMS

A set of computer programs has been written for use in the analysis of microwave radiometry. The main programs are:

- o Skytemp
- o Pathtemp
- o Emis

The first program, Skytemp, performs the integration of specific attenuations to obtain the radiometric sky temperature at various incidence angles. It assumes a flat earth and a layered atmosphere, and assumes that all significant attenuation occurs in the first 10Km of atmosphere. Thermometric temperatures and specific attenuations are read from files pre-stored on the H-6080 disk file system, and sky temperatures are output to the disk on a file names FLTSKY in a format which is easy for the computer to use in further calculations.

Pathtemp is a very similar program, which integrates the specific attenuation to obtain the total one way attenuation on any glide path from any altitude to the ground. It also computes the path emission observed at any altitude (under 10Km) and at depression angles from .01745 rad to .157 rad (1° to 9°), for the ILM weather cases. Its output is to a disk file named FLTPATH for path temperature or FLATRANS for path attenuation.

Program Skytemp

```
      DIMENSION ALPHA(28,10),THIK(28),THED(18),TSKY(18,10),TEMP(28,10)
      DATA THIK/20*.1,8*1./
      CALL ATTACH(20,'D00048/FLALPHA;',3,0,IS,)
      CALL ATTACH(21,'D00048/FLTEMP;',3,0,ISTAT,)
      REWIND 20
      REWIND21
      READ(20,241,END=49)((ALPHA(I,J),I=1,28),J=1,10)
   49 READ(21,242,END=50)((TEMP(I,J),I=1,28),J=1,10)
   50 DO 200 K=1,18
      IF(K.GE.10) GO TO 100
      THED(K)=K
      THETA=K/57.29
      GO TO 120
  100 THED(K)=K-9
      THETA=THED(K)/5.729
  120 CONTINUE
      SINTH=SIN(THETA)
      DO 190 L=1,10
      IF(K.NE.1)GO TO 145
  145 CONTINUE
    6 ATTENJ=1.
      TSKY(K,L)=0.0
      DO 190 I=1,28
      ATTENI=ATTENJ*EXP(-.23*ALPHA(I,L)*THIK(I)/SINTH)
      TSKY(K,L)=TSKY(K,L)+(200.+TEMP(I,L))*(ATTENJ-ATTENI)
      ATTENJ=ATTENI
  190 CONTINUE
  200 CONTINUE
      CALL ATTACH(22,'D00048/FLTSKY;',3,0,ISTAT,)
      REWIND22
      WRITE(22,240)((TSKY(I,J),I=1,18),J=1,10)
  240 FORMAT(6E12.4)
  241 FORMAT(2(10E12.4/),8E12.4)
  242 FORMAT(14F4.2)
      CALL DETACH(20,IS,)
      CALL DETACH(21,IS,)
      CALL DETACH(22,IS,)
      STOP
      END
```

```
      DIMENSION GAMSUM(2,18),REFOUT(18),GLTMP(10),EMSV(2),SPEC(2),SPSKY(10)
      DIMENSION SPCSKY(9,10)
      DIMENSION TSKY(9,10),WXCS(10),TD(10,2)
      DIMENSION TAPP(10,2),TSPEC(10,2),TEMIT(10,2),EMIT(2)
      DATA RGH,SLP,PRMRE,PRMIM/.5,.3,.2,10.,10./
       DATA GLTMP/295.,8*282.7,268./
       CALL ATTACH(21,'D00048/OUTPUT;',3,0,IS,)
       REWIND 21
       DATA DINC/89./
      CALL ATTACH(20,'D00048/FLTSKY;',3,0,ISTAT,)
      REWIND 20
       READ(20,34)((SPCSKY(I,J),I=1,9),(TSKY(K,J),K=1,9),J=1,10)
   34  FORMAT(6F12.4)
  040 PRINT 36
  036 FORMAT('ROUGH SURFACE PARAMETERS,RGH,SLP,PRMRE,PRMIM')
       READ 38,DAT1,DAT2,DAT3,DAT4
  038 FORMAT(4F8.4)
       KSPEC=90-DINC
       AINC=DINC/57.29
       IF(DAT1.EQ.0.)GO TO 43;RGH=DAT1;SLP=DAT2;PRMRE=DAT3;PRMIM=DAT4
      DATA WXCS/1.0,2.1,2.2,2.3,2.4,3.1,3.2,3.3,3.4,4.0/
  043 EMIT2=0.
       RUM=100.0
       EMIT1=0.0
       DO 425 J=1,18
       GAMSUM(1,J)=0.
       GAMSUM(2,J)=0.
       REFOUT(J)=10*J-95
       AREFL=REFOUT(J)/57.29
       DO 420 I=1,9
       AOAZ=(I-1)/5.729
       CSINC=COS(AINC)
       CSREF=COS(AREFL)
       CSOAZ=COS(AOAZ)
       SNINC=SIN(AINC)
       SNREF=SIN(AREFL)
       SNOAZ=SIN(AOAZ)
       A2=(CSINC*SNREF+SNINC*CSREF*CSOAZ)**2
       A3=(SNINC*CSREF+CSINC*SNREF*CSOAZ)**2
       A5=SNINC*SNREF*CSOAZ-CSINC*CSREF
       CSLIN=(1.-A5)/2.
       SNLIN=(1.+A5)/2.
       CALL ERSNCL(SNLIN,CSLIN,PRMRE,PRMIM,RV,RH)
       ESAM=A2*(A3+(SNREF*SNOAZ)**2)/((1+A5)**2)
       ECRS=(SNINC*SNOAZ)**2*(A3+SNOAZ**2)/((1+A5)**2)
       EXYSQ=SNINC**2+SNREF**2-2*SNINC*SNREF*CSOAZ
       G=(6.283*RGH*(CSINC+CSREF))**2
       IF(G.LT.12.5) GO TO 377
C      ****VERY ROUGH EXPONENTIAL****
       TEMP1=G**2+39.474*SLP**2*EXYSQ
       REST=78.956*G*SLP**2/((CSINC+CSREF)**2*TEMP1*SQRT(TEMP1))
       GO TO 400
C      ****SLIGHTLY ROUGH EXPONENTIAL****
  377 SUMG=0.0
       SMLST=0.
       FACTM=1.
       GTOM=1.
```

```
790 470 FORMAT("THETA?   VERTICAL    HORIZONTAL")
800 480 FORMAT(F5.1,4X,F11.4,1X,F11.4)
810 695 FORMAT(10(2X,F3.1,4(5X,F5.1),7X,4(5X,F5.1)/))
825 825 FORMAT("WEATHER",2X,"RHODIFFUSE ",2X,"RHSPECULAR",2X,"RHEMITTED ",2X,
826&     "RHAPPARENT",10X,"RHDIFFUSE ",2X,"RHSPECULAR",2X,"RHEMITTED ",2X,"RHAPPARENT")
827 826 FORMAT(" CASE",6X,"THSKY",7X,"THSKY",15X,"TEMPERATURE",10X,"THSKY",
828&     7X,"THSKY",15X,"TEMPERATURE"/10X,"VERTICAL POLARIZATION",20X,
829&     20X,"HORIZONTAL POLARIZATION")
830      READ 482,QINC
840 482 FORMAT(F10.4)
850      IF(QINC.NE.0.)GO TO 40
851      CALL DETACH(20,ISTAT,)
852      CALL DETACH(21,ISTAT,)
858      CALL DETACH(21,IS,)
860 STOP
870 END
880  FUNCTION SHAD(SLOP,TANA)
890      THET=SLOP/TANA
900      EPFC=.5/((1+.278393*THET+.230389*THET**2+.000972*THET**3+.078108*
9106&          THET**4)**4)
920      SHAD=EXP(-.5*TANA*EPFC)
930 870 RETURN
940 880 FORMAT("SHADOWING QUESTIONABLE)
950   END
1000 SUBROUTINE FRSNEL(SNLIN,CSLIN,PRMRE,PRMIM,RV,RH)
1010      B1=PRMRE-SNLIN
1020      A6SQ=SQRT(B1**2+PRMIM**2)
1030      B2=.5*ATAN2(PRMIM/B1)
1040      CSB=COS(B2)
1050      SNB=SIN(B2)
1060      PNORM=PRMRE**2+PRMIM**2
1070      RV=((PNORM*CSLIN)**2+4*A6SQ*(PRMRE*SNB)**2*CSLIN+A6SQ**2-2*
10806&         A6SQ*PNORM*CSLIN)/((PNORM*CSLIN+2*
1090 &         SQRT(A6SQ*CSLIN)*(PRMRE*CSB+PRMIM*SNB)+A6SQ)**2)
1100      CONTINUE
1110      RH=(CSLIN**2+A6SQ*4*SNB**2*CSLIN+A6SQ**2-2*A6SQ*CSLIN)/((CSLIN+
11206&         2*SQRT(
1130 &      A6SQ*CSLIN)*CSB+A6SQ)**2)
1140      RETURN
1150      END
```

SURFACE PARAMETERS: ROUGHNESS= 0.084 CORRELATION LENGTH= 0.20 PERMITIVITY= 5.5+J 0.5 INCIDENCE ANGLE=86.0

WEATHER CASE	DIFFUSE SKY	SPECULAR SKY	EMITTED	APPARENT TEMPERATURE	DIFFUSE SKY	SPECULAR SKY	EMITTED	APPARENT TEMPERATURE
	VERTICAL POLARIZATION				HORIZONTAL POLARIZATION			
1.0	3.8	53.0	239.1	294.8	3.3	205.0	86.3	294.7
2.1	0.4	23.9	229.2	252.5	0.3	92.6	82.7	175.7
2.2	0.4	24.2	229.2	252.7	0.3	93.5	82.7	176.6
2.3	0.4	27.0	228.2	255.6	0.4	104.4	82.7	187.5
2.4	0.6	33.8	229.2	262.6	0.6	130.8	82.7	214.1
3.1	1.5	47.8	229.2	277.4	1.3	185.0	82.7	269.0
3.2	1.5	48.0	229.2	277.6	1.3	185.8	82.7	269.8
3.3	1.8	49.7	229.2	279.6	1.6	192.2	82.7	276.5
3.4	2.3	50.7	229.2	281.2	2.1	196.2	82.7	281.0
4.0	0.3	20.4	216.3	237.0	0.3	78.8	78.4	157.5

SURFACE PARAMETERS: ROUGHNESS= 0.084 CORRELATION LENGTH= 0.20 PERMITIVITY= 5.5+J 0.5 INCIDENCE ANGLE=84.0

WEATHER CASE	DIFFUSE SKY	SPECULAR SKY	EMITTED	APPARENT TEMPERATURE	DIFFUSE SKY	SPECULAR SKY	EMITTED	APPARENT TEMPERATURE
	VERTICAL POLARIZATION				HORIZONTAL POLARIZATION			
1.0	9.3	45.2	240.1	294.7	8.2	188.0	98.2	294.4
2.1	0.9	15.1	230.1	246.1	0.9	62.7	94.1	157.6
2.2	0.9	15.2	230.1	246.3	0.8	63.4	94.1	158.3
2.3	1.1	17.3	230.1	248.4	0.9	71.8	94.1	166.9
2.4	1.5	22.5	230.1	254.1	1.3	93.7	94.1	189.1
3.1	3.5	37.8	230.1	271.4	3.1	157.2	94.1	254.4
3.2	3.6	38.1	230.1	271.7	3.2	158.3	94.1	255.6
3.3	4.2	40.6	230.1	274.9	3.6	169.7	94.1	266.6
3.4	5.7	43.0	230.1	279.7	5.0	178.5	94.1	277.7
4.0	0.7	12.7	218.1	231.6	0.7	52.6	89.2	142.6

SURFACE PARAMETERS: ROUGHNESS= 0.100 CORRELATION LENGTH= 1.00 PERMITIVITY= 3.2+J85.0 INCIDENCE ANGLE=89.0

WEATHER CASE	DIFFUSE SKY	SPECULAR SKY	EMITTED	APPARENT TEMPERATURE	DIFFUSE SKY	SPECULAR SKY	EMITTED	APPARENT TEMPERATURE
	VERTICAL POLARIZATION				HORIZONTAL POLARIZATION			
1.0	0.0	3.7	290.0	293.7	0.0	283.2	10.6	293.8
2.1	0.0	3.2	277.9	281.1	0.0	246.5	10.2	256.7
2.2	0.0	3.2	277.9	281.1	0.0	247.4	10.2	257.6
2.3	0.0	3.3	277.9	281.2	0.0	256.0	10.2	266.2
2.4	0.0	3.5	277.9	281.4	0.0	267.4	10.2	277.5
3.1	0.0	3.5	277.9	281.4	0.0	268.2	10.2	278.4
3.2	0.0	3.5	277.9	281.4	0.0	268.8	10.2	279.0
3.3	0.0	3.5	277.9	281.4	0.0	271.0	10.2	281.2
3.4	0.0	3.5	277.9	281.4	0.0	271.4	10.2	281.6
4.0	0.0	3.0	263.4	266.4	0.0	226.3	9.6	235.9

SURFACE PARAMETERS: ROUGHNESS= 0.100 CORRELATION LENGTH= 1.00 PERMITIVITY= 3.2+J85.0 INCIDENCE ANGLE=84.0

WEATHER CASE	DIFFUSE SKY	SPECULAR SKY	EMITTED	APPARENT TEMPERATURE	DIFFUSE SKY	SPECULAR SKY	EMITTED	APPARENT TEMPERATURE
	VERTICAL POLARIZATION				HORIZONTAL POLARIZATION			
1.0	46.9	88.5	158.0	293.5	49.9	262.1	0.	312.0
2.1	4.6	29.5	151.4	185.6	4.7	87.4	0.	92.1
2.2	4.7	29.9	151.4	186.0	4.8	88.3	0.	93.1
2.3	5.4	33.8	151.4	190.7	5.5	100.1	0.	105.6
2.4	7.5	44.1	151.4	203.1	7.7	130.6	0.	138.3
3.1	17.8	74.0	151.4	243.3	18.4	219.1	0.	237.5
3.2	18.1	74.6	151.4	244.1	18.7	220.7	0.	239.4
3.3	21.5	79.5	151.4	252.4	22.2	235.2	0.	257.4
3.4	28.8	94.1	151.4	264.3	30.0	248.9	0.	278.9
4.0	3.8	24.8	143.6	172.2	3.9	73.4	0.	77.3

SURFACE PARAMETERS: ROUGHNESS= 0.500 CORRELATION LENGTH= 3.20 PERMITIVITY= 10.0+J10.0 INCIDENCE ANGLE=86.0

WEATHER CASE	DIFFUSE SKY	SPECULAR SKY	EMITTED	APPARENT TEMPERATURE	DIFFUSE SKY	SPECULAR SKY	EMITTED	APPARENT TEMPERATURE
	VERTICAL POLARIZATION				HORIZONTAL POLARIZATION			
1.0	45.9	15.2	232.4	293.5	51.2	198.6	43.3	293.1
2.1	4.3	6.8	222.7	233.9	4.4	89.7	41.5	135.5
2.2	4.4	6.9	222.7	234.0	4.4	90.6	41.5	136.4
2.3	5.0	7.7	222.7	235.5	5.1	101.1	41.5	147.6
2.4	7.0	9.7	222.7	239.4	7.1	126.7	41.5	175.3
3.1	16.8	13.7	222.7	253.2	17.3	179.2	41.5	238.0
3.2	17.1	13.7	222.7	253.5	17.6	179.9	41.5	239.0
3.3	20.3	14.2	222.7	257.3	21.1	186.2	41.5	248.7
3.4	27.4	14.5	222.7	264.7	28.9	190.0	41.5	260.4
4.0	3.6	5.8	211.1	220.5	3.6	76.3	39.3	119.2

SURFACE PARAMETERS: ROUGHNESS= 0.500 CORRELATION LENGTH= 3.20 PERMITIVITY= 10.0+J10.0 INCIDENCE ANGLE=84.0

WEATHER CASE	DIFFUSE SKY	SPECULAR SKY	EMITTED	APPARENT TEMPERATURE	DIFFUSE SKY	SPECULAR SKY	EMITTED	APPARENT TEMPERATURE
	VERTICAL POLARIZATION				HORIZONTAL POLARIZATION			
1.0	105.9	13.9	172.1	291.9	122.1	149.3	19.5	290.9
2.1	9.6	4.6	164.9	179.1	9.9	49.8	18.7	78.4
2.2	9.7	4.7	164.9	179.3	10.1	50.3	18.7	79.1
2.3	11.2	5.3	164.9	181.5	11.6	57.0	18.7	87.3
2.4	15.6	6.9	164.9	187.5	16.2	74.4	18.7	109.3
3.1	37.7	11.6	164.9	214.2	39.9	124.8	18.7	183.4
3.2	38.3	11.7	164.9	214.9	40.6	125.7	18.7	185.0
3.3	45.7	12.5	164.9	223.0	48.7	134.0	18.7	201.3
3.4	61.9	13.2	164.9	240.1	67.2	141.8	18.7	227.7
4.0	7.9	3.9	156.3	168.1	8.2	41.8	17.7	67.7

PATH TEMPERATURES

RANGE= 2 KM.

WEATHER CASE	GLIDE SLOPE=1 DEG.	2 DEG.	3 DEG.	4 DEG.	5 DEG.	6 DEG.	7 DEG.	8 DEG.	9 DEG.
1.0	102.725	195.691	256.728	249.288	252.112	257.123	254.932	256.017	257.161
2.1	11.260	11.601	11.560	10.795	10.349	10.038	9.777	9.595	9.422
2.2	14.251	14.806	14.689	13.152	12.240	11.618	11.133	10.774	10.481
2.3	44.589	51.238	51.665	41.563	35.307	31.036	27.906	25.538	23.670
2.4	84.661	122.958	135.410	110.676	93.903	81.819	72.691	65.583	59.883
3.1	13.062	13.526	13.649	13.576	13.568	13.557	13.512	13.491	13.465
3.2	17.941	18.840	19.095	19.026	19.054	19.074	19.048	19.051	19.049
3.3	60.574	74.714	79.513	78.811	79.623	80.314	80.266	80.664	80.973
3.4	94.740	157.891	189.072	194.270	187.385	190.862	189.727	191.069	192.161
4.0	5.540	5.624	5.640	5.596	5.576	5.555	5.521	5.497	5.471

RANGE= 8

WEATHER CASE	GLIDE SLOPE=1 DEG.	2 DEG.	3 DEG.	4 DEG.	5 DEG.	6 DEG.	7 DEG.	8 DEG.	9 DEG.
1.0	294.274	293.660	293.074	292.499	291.928	291.372	290.809	290.243	289.674
2.1	33.250	29.035	27.308	26.215	25.381	24.682	24.064	23.499	22.972
2.2	41.783	33.411	30.254	28.438	27.168	26.176	25.349	24.627	23.978
2.3	129.343	83.160	65.073	55.228	49.951	44.542	41.233	38.629	36.503
2.4	242.680	181.093	143.934	120.399	104.288	92.571	83.648	76.607	70.894
3.1	38.932	38.714	38.471	38.223	39.255	43.767	46.983	49.407	51.311
3.2	53.374	53.377	53.327	53.264	53.732	55.669	57.088	58.184	59.069
3.3	176.709	178.256	179.358	180.313	177.893	164.402	153.723	145.105	138.029
3.4	271.883	272.104	272.186	272.185	271.224	264.792	257.640	250.234	242.874
4.0	16.554	16.315	16.073	15.834	15.599	15.367	15.137	14.909	14.685

RANGE=16

WEATHER CASE	GLIDE SLOPE=1 DEG.	2 DEG.	3 DEG.	4 DEG.	5 DEG.	6 DEG.	7 DEG.	8 DEG.	9 DEG.
1.0	293.836	292.050	290.272	288.514	286.783	285.067	283.496	283.043	282.785
2.1	68.005	62.079	58.316	55.178	52.340	49.702	47.360	45.234	43.549
2.2	75.343	65.879	60.899	57.145	53.935	51.047	48.525	46.264	44.472
2.3	149.794	109.086	91.430	80.851	73.380	67.579	62.929	59.046	55.962
2.4	248.136	194.143	160.576	138.519	122.777	110.813	101.392	93.715	87.511
3.1	91.203	96.161	113.083	121.289	126.271	129.717	132.240	132.768	133.977
3.2	120.352	122.562	129.436	133.064	135.433	137.192	138.543	138.269	138.829
3.3	261.107	258.745	239.881	225.165	214.014	205.476	198.824	192.740	188.216
3.4	281.513	280.240	279.265	276.821	273.082	268.521	263.645	258.622	253.793
4.0	40.876	39.380	37.900	36.457	35.063	33.729	32.563	31.530	30.740

APPENDIX F

MLS CONFIGURATION K AIRBORNE EQUIPMENT

PHYSICAL DESCRIPTION OF FAA-K AIRBORNE EQUIPMENT

The H-80 Airborne Equipment Set offers operational and installation flexibility through compact, modular equipment packaging.

The H-80 airborne system will meet all FAA-K equipment requirements. Figure F-1 shows two airborne sets in a typical redundant aircraft installation. Features include a standardized package design and simplified interconnections that will permit straightforward installation of the equipment in the DC-6 or CV-880 aircraft. When the airborne equipment is used in the dual configuration illustrated, provisions are made for interconnection of the two HN-700 Angle Receiver/Processors to implement built-in cross monitoring capability.

The physical characteristics of each H-80 subsystem are summarized below and discussed in detail in the following paragraphs.

Physical Characteristics of H-80 Equipment Set

	Angle Rec/Proc (HN-700)	DME Interr. (HN-800)	Control Unit (HC-400)	Antennas	
				(HL-181)	(HL-362) (HL-363)
Size	3/4 ATR Long	1/2 ATR Short	5.75"W, 4.125"H, 2.5"D	4"H, 5"W, 6"D	Not Defined " "
Weight	20 lbs	10 lbs	3 lbs	1 lb	Not Defined
Power	145 w	40 w	15 w	--	--

Although the HR-800 DME Interrogator is considered an integral subsystem, the HN-700 Angle Receiver/Processor can operate independently.

The H-80 airborne set is designed to use about 200 watts of 400 Hz, single phase, 115v aircraft power. The HN-700 connects to the aircraft power source and supplies the required dc power to the other units as required.

The airborne units have been designed for hard-mounting in the aircraft, and will operate and withstand expected prototype aircraft environmental conditions:

Temperatures -40 degrees to +65 degrees C

Vibration +2 g's per MIL-STD-810B (Curve B, Figure 514-1)

The HN-700 is packaged in a standard 3/4 ATR long case and has been dimensioned for hard mounting to the test aircraft equipment rack for ease of installation. Mechanical holddown clamps allow quick installationand removal of equipment. Plug-in circuit boards allow fast replacement of defective circuits for ease of maintenance.

System interconnections have been simplified and provide ready access to connectors and test points for in-flight equipment monitoring during the test program. These connectors, as well as the test point access, are located on the front panel. The HN-700 interconnects to the HC-500 control unit for channel select and azimuth and elevation path selection. Additionally, The HN-700 provides basic low dc voltages, RF signal down conversion, and a frequency synthesizer signal for the HR-800. The HN-700 angle deviation outputs are scaled to standard ILS course width sensitivities and are therefore compatible with the existing set of avionics in the test aircraft.

PERFORMANCE CHARACTERISTICS OF FAA-K AIRBORNE EQUIPMENT

The performance characteristics of the configuration K-FAA Airborne Doppler MLS Equipment Set, designated H-80, will meet the FAA requirements for high-capability guidance equipment for aircraft engaged in autoland operations at primary hub airports.

The H-80 airborne equipment has been designed to provide precise takeoff and landing terminal area guidance information, under Category III weather conditions, for fixed-wing civil aircraft operating with autoland avionics at suitably equipped major runways. The airborne set will provide the accuracies and functional characteristics in Tables F-1 and F-2.

The HN-700 provides the 200 channel frequency synthesizer, down conversion of both the angle guidance and DME, as well as the signal processing for the angle data. The accuracy of the angle guidance information is preserved even under heavy multipath conditions by the use of a digitally implemented, matched tracking filter that acquires and tracks the direct signal. In acquiring the angle data, the processor employs a search algorithm that prevents lock-on to bright flashes or other spurious signals. Once in track, the receiver verification circuitry continuously checks the video spectrum to assure that the tracked signal is the correct one. In case of failure to verify, the receiver is forced to re-acquire the signal.

Table F-2. Specific Performance Features of Configuration K, FAA Airborne Equipment

Item	Description
Lateral Path	
Azimuth Select	Pilot select of ±30 deg in 5-degree increments
Sensitivity	ILS compatible deviation with course softening option within desired range.
Wide Angle	±60 degree suitable for display.
Missed Approach	Automatic front-to-back AZ switching with DME.
Vertical Path	
Glidepath Select	2 to 12 degrees in 0.5-degree increments
Sensitivity	ILS compatible, with course softening option within desired range.
Coordinates	Conical, with option of EL1 planar equivalent through DME algorithm.
Flare Altitude and Rate	Suitable for Collins 860F-1 display and 11SA435 A flare coupler.
Range and Range Rate	Suitable for Collins 860-3 digital DME indicator.
Monitoring	On-line monitoring, self-monitoring push-to-test confidence test. Comparison test.
Altitude/Range Discretes	Marker beacon, flare, and decrab options.

pushbutton and MLS subsystem status lights which are activated by the self-monitoring circuitry in the MLS equipment. The HN-400 control panel further provides access to the HN-700 microprocessor programming, wherein certain operational options may be implemented. For example, although normal Elevation 1 output is conical, both deviation and total angle may be converted to a planar equivalent through keyboard entry of proper coding to implement an appropriate DME conversion algorithm.

The HL-362 and HL-363 omnidirectional antennas are provided to assure full MLS airborne antenna coverage during the diverse aircraft maneuvers associated with curved approach paths, missed approach, and departures. The HL-181 sector horn antenna provides effective gain enhancement of the guidance signals, as well as assuring adequate coverage for the critical final approach phase of the terminal area mission.